The Plant Cell, Vol. 26: 650–664, February 2014, www.plantcell.org

STENOFOLIA Recruits TOPLESS to Repress *ASYMMETRIC LEAVES2* at the Leaf Margin and Promote Leaf Blade Outgrowth in *Medicago truncatula*[C][W]

Fei Zhang,[a] Yewei Wang,[a] Guifen Li,[b] Yuhong Tang,[b] Elena M. Kramer,[c] and Million Tadege[a,1]

[a] Department of Plant and Soil Sciences, Institute for Agricultural Biosciences, Oklahoma State University, Ardmore, Oklahoma 73401
[b] Plant Biology Division, The Samuel Roberts Noble Foundation, Ardmore, Oklahoma 73401
[c] Department of Organismic and Evolutionary Biology, Harvard University, Cambridge, Massachusetts 02138

The *Medicago truncatula WUSCHEL*-related homeobox (*WOX*) gene, *STENOFOLIA* (*STF*), plays a key role in leaf blade outgrowth by promoting cell proliferation at the adaxial-abaxial junction. *STF* functions primarily as a transcriptional repressor, but the underlying molecular mechanism is unknown. Here, we report the identification of a protein interaction partner and a direct target, shedding light on the mechanism of *STF* function. Two highly conserved motifs in the C-terminal domain of STF, the WUSCHEL (WUS) box and the STF box, cooperatively recruit TOPLESS (Mt-TPL) family corepressors, and this recruitment is required for STF function, as deletion of these two domains (STFdel) impaired blade outgrowth whereas fusing Mt-TPL to STFdel restored function. The homeodomain motif is required for direct repression of *ASYMMETRIC LEAVES2* (Mt-*AS2*), silencing of which partially rescues the *stf* mutant phenotype. *STF* and *LAMINALESS1* (*LAM1*) are functional orthologs. A single amino acid (Asn to Ile) substitution in the homeodomain abolished the repression of Mt-*AS2* and STF's ability to complement the *lam1* mutant of *Nicotiana sylvestris*. Our data together support a model in which STF recruits corepressors to transcriptionally repress its targets during leaf blade morphogenesis. We propose that recruitment of TPL/TPL-related proteins may be a common mechanism in the repressive function of modern/WUS clade *WOX* genes.

INTRODUCTION

Leaf primordia are determinate lateral organs initiated from a small group of pluripotent stem cells in the shoot apical meristem. After primordium initials are recruited from the shoot apical meristem, the primordium organizes itself into defined cell layers through highly regimented cell division and cell differentiation patterns, forming a flat lamina (blade) that develops along three distinct axes: proximal-distal, medial-lateral, and adaxial-abaxial. Despite tremendous progress, how such a highly organized structure develops from undifferentiated stem cells remains a fundamental question in plant developmental biology.

Polarity patterning along the adaxial-abaxial axis of the leaf blade is required for blade outgrowth (Waites and Hudson, 1995; McConnell and Barton, 1998; Bowman et al., 2002; Efroni et al., 2010; Byrne, 2012), and the genetic determinants of polarity have been well defined in the model plant *Arabidopsis thaliana* (Waites et al., 1998; Byrne et al., 2000; Kerstetter et al., 2001; McConnell et al., 2001; Emery et al., 2003; Juarez et al., 2004). It is well established that adaxial and abaxial polarity factors interact in a mutually antagonistic manner to maintain domain specificity and allow cell differentiation in their respective domains (Bowman et al., 2002; Tsukaya, 2006; Husbands et al., 2009; Efroni et al., 2010). The adaxial polarity factor *ASYMMETRIC LEAVES2* (*AS2*) is proposed to prevent cell proliferation in the adaxial domain (Iwakawa et al., 2007) in addition to maintaining adaxial polarity by regulating the patterns of miR165/166 distribution (Ueno et al., 2007). AS2 forms a repressive complex with AS1 and prevents meristematic activity in leaves by directly repressing the transcription of *KNOTTED1*-like homeobox (*KNOX*) genes (Guo et al., 2008; Luo et al., 2012). The AS1/AS2 complex has also recently been shown to directly or indirectly repress the abaxial factors *ETTIN/AUXIN RESPONSE FACTOR3* (*ARF3*) and *ARF4* (Iwasaki et al., 2013). The repression of *KNOX* genes in leaves by the AS1/AS2 complex is required not only for proper differentiation of leaf cells but also for the commitment of leaf founder initial cells to form a leaf primordium, where the down-regulation *KNOX* genes at the incipient primordium site is required for leaf initiation (Hake et al., 2004; Moon and Hake, 2011). The AS1/AS2 complex interacts with the histone chaperone HIRA (Phelps-Durr et al., 2005) and the Polycomb-repressive complex2 for the repression of *KNOX* genes (Lodha et al., 2013). These observations indicate that leaf primordium initiation and elaboration involves stable repression of shoot apical meristem programs by the AS1/AS2 complex and chromatin-remodeling factors maintaining a transcriptionally repressed chromatin state. However, how preventing cell proliferation alone or in combination with the promotion of cell differentiation by the AS1/AS2 complex or other polarity factors mediates blade outgrowth is unclear. Moreover, as the primordium grows away from the meristem, physical recruitment of meristematic cells from the shoot apical meristem becomes unfeasible, and the leaf founder initial cells could become limiting for leaf growth. This

[1] Address correspondence to million.tadege@okstate.edu.
The author responsible for distribution of materials integral to the findings presented in this article in accordance with the policy described in the Instructions for Authors (www.plantcell.org) is: Million Tadege (million.tadege@okstate.edu).
[C] Some figures in this article are displayed in color online but in black and white in the print edition.
[W] Online version contains Web-only data.
www.plantcell.org/cgi/doi/10.1105/tpc.113.121947

suggests that there may be a need for the maintenance of undifferentiated cells in the determinate leaf primordium during leaf morphogenesis and elaboration. At the adaxial-abaxial boundary of the leaf primordium, the marginal blastozone (Hagemann and Gleissberg, 1996), previously termed the marginal meristem, would be a potential site for such undifferentiated cells, but it is difficult to imagine how such meristematic cells could be maintained while class I *KNOX* genes, including *SHOOT MERISTEMLESS*, *BREVIPEDICELLUS* (*KNAT1*), *KNAT2*, and *KNAT6*, are stably repressed.

Recently, a third domain, located at the adaxial-abaxial junction of the lamina, was found to be required for cell proliferation–mediated blade outgrowth (Tadege et al., 2011a; Nakata et al., 2012). The identity of this inner (middle) domain is regulated by the WUSCHEL-related homeobox (WOX) family homeodomain (HD) transcription factor *STENOFOLIA* (*STF*) in *Medicago truncatula* and its orthologs in other dicots, including *MAEWEST* in *Petunia* × *hybrida* (Vandenbussche et al., 2009), *LAM1* in *Nicotiana sylvestris* (Tadege et al., 2011a), *WOX1* and *PRESSED FLOWER* (*PRS*) in *Arabidopsis* (Vandenbussche et al., 2009; Nakata et al., 2012), and *LATHYROIDES* in pea (*Pisum sativum*) (Zhuang et al., 2012). The diagnostic phenotype of *stf* and *lam1* mutants is dramatic reduction in leaf width with no significant effect on leaf length. This defect results from reduced cell proliferation in the lateral direction (Tadege et al., 2011a; Nakata et al., 2012) and is most dramatically exhibited in the *lam1* mutant of *N. sylvestris* (McHale, 1992), where the phenotype is so severe that, essentially, the main visible structure of the leaf is the midrib with vestigial blade strips. The involvement of *WOX* genes in leaf blade outgrowth has been demonstrated in maize (*Zea mays*), where two duplicate *WOX* genes, *narrowsheath1* (*ns1*) and *ns2*, were shown to redundantly regulate blade outgrowth (Nardmann et al., 2004). Similarly, in rice (*Oryza sativa*), the orthologs of *ns1* and *ns2* are shown to be involved in leaf blade outgrowth (Cho et al., 2013), suggesting that the requirement for WOX function in leaf blade development is conserved in both dicots and monocots. However, the dicot genes *STF/WOX1* are not necessarily the orthologs of *ns1* and *ns2*, as these are represented by *PRS/WOX3* in dicots, and the *STF/WOX1* lineage appears to have no homologs in monocots (Tadege et al., 2011a, 2011b).

STF acts mainly as a transcriptional repressor, and the evolutionarily conserved WUS box, which is specific to the modern/WUS clade *WOX* genes, partially contributes to this repressive activity (Lin et al., 2013). These findings established that the *STF*-mediated transcriptional repression is central to cell proliferation at the adaxial-abaxial junction that regulates blade outgrowth and showed that this activity may be shared by other WUS clade *WOX* genes involved in cell proliferation, including *WUS* and *WOX5* (Lin et al., 2013). This interpretation is consistent with the reports of Kieffer et al. (2006) and Ikeda et al. (2009), who proposed that *WUS* mainly acts as a repressor in meristem stem cell maintenance. However, the molecular mechanism underlying the repressive activity of STF in leaf development is unknown. Neither the targets of STF repression nor the interacting partners that are required for STF activity have been identified.

In this study, we show that *M. truncatula* STF physically interacts with the corepressor TOPLESS (Mt-TPL) by its WUS box and STF box and that this interaction is required for both leaf blade development and the repression of Mt-*AS2* at the leaf margin, suggesting that the STF-TPL repressor complex promotes cell proliferation by preventing the activity of *AS2*.

RESULTS

The HD and the C-Terminal Domain of STF Are Essential for Leaf Blade Outgrowth Function

To explore how the *M. truncatula* STF protein functions as a transcription factor, we performed amino acid sequence alignment of STF proteins from different species. Based on the conserved domain analysis, we divided the STF protein into four major parts: the N-terminal domain (NTD; amino acids 1 to 90), HD (amino acids 91 to 163), middle domain (MD; amino acids 164 to 300), and C-terminal domain (CTD; amino acids 301 to 358), which contains two highly conserved motifs, the WUS box (amino acids 309 to 318) and the STF box (amino acids 349 to 358) (Figure 1A; Supplemental Figure 1).

To evaluate the functions of these domains, we performed individual and combined domain deletions and introduced the truncated forms, driven by a 2.66-kb *STF* promoter (Tadege et al., 2011a), into the *lam1* mutant of *N. sylvestris*, an invaluable genetic tool for functional analysis (Figure 1B). Compared with the wild-type *STF* gene, which fully complemented the *lam1* mutation (Figure 1C), truncation of the NTD or MD resulted in a partial reduction of the ability of *STF* to rescue *lam1*, leading to slightly narrowed leaves with wavy margins (Figures 1D and 1E). Deletion of both the NTD and MD resulted in weaker *lam1* complementation with more pronounced leaf narrowing and increased waviness of the margins (Figure 1F), indicating that the NTD and MD may have redundant functions in leaf development. However, deletion of both of these domains fails to fully abolish *STF* function, suggesting that their roles are not critical. By contrast, deletion of either the HD (Figure 1G) or the CTD (Figure 1H) completely abolished the ability of *STF* to complement *lam1*, indicating that DNA binding ability and interactions via the CTD are indispensable to *STF* function.

Both the WUS Box and the STF Box of the CTD Are Required for STF-Repressive Function

Since truncated *STF* lacking the CTD completely failed to rescue *lam1*, we compared the individual contributions of the WUS box and STF box to STF activity. We first examined the transcriptional activity of STF and its CTD-deleted mutant (STFdel) by transient luciferase expression protoplast assays (Figures 2A to 2C). While expression of the intact STF protein repressed the expression of the reporter gene construct by more than 2-fold compared with the empty effector plasmid, STFdel showed little, if any, repressive activity (Figure 2C). We next examined whether the conserved WUS box and STF box in the CTD contribute to the repressive activity by substitution of Leu with Ala in the individual WUS box and STF box motifs (Figure 2B). Consistent with our previous report (Lin et al., 2013), mutation of the WUS box (m1) partially relieved the repression of reporter gene expression by STF. Likewise, mutation of the STF box (m2) also resulted in the partial loss of reporter gene repression. However, mutations in both WUS box and STF box (m1m2) almost fully abolished STF repression, similar

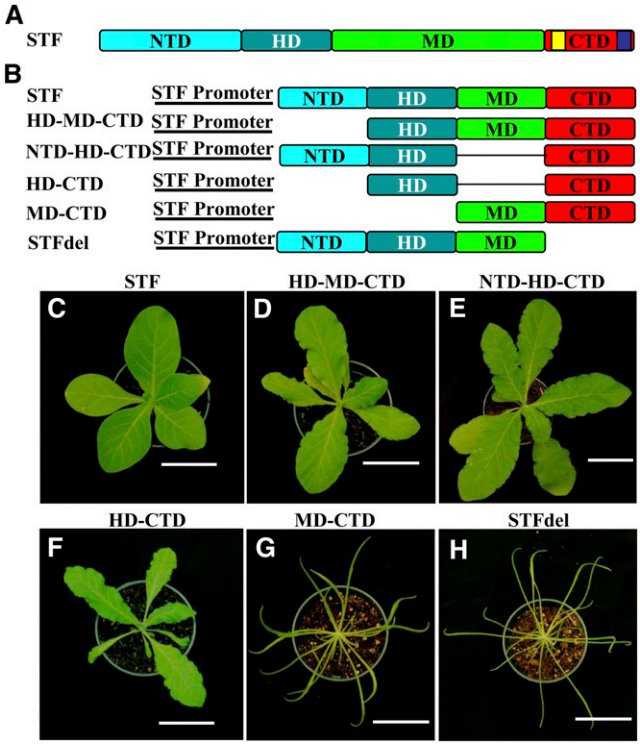

Figure 1. The HD and CTD of STF Are Essential for Blade Outgrowth Function.

(A) Schematic representation of domain arrangements in STF protein from the N terminus to the C terminus. Domains are as follows: NTD, amino acids 1 to 90; HD, amino acids 91 to 163; MD, amino acids 164 to 300; CTD, amino acids 301 to 358. The CTD contains two conserved motifs: the WUS box (yellow; amino acids 309 to 318, QTLQLFPIRN) and the STF box (blue; amino acids 349 to 358, QFIEFLPLKN).

(B) Constructs used in the deletion assay for complementation of the *N. sylvestris lam1* mutant. All constructs were driven by the *M. truncatula STF* promoter.

(C) to **(H)** Complementation of *N. sylvestris lam1* by deletion mutant constructs of the *M. truncatula STF* gene. The *lam1* mutants were transformed with *STF:STF* **(C)**, *STF:HD-MD-CTD* **(D)**, *STF:NTD-HD-CTD* **(E)**, *STF:HD-CTD* **(F)**, *STF:MD-CTD* **(G)**, and *STF:STFdel* **(H)**. Bars = 5 cm.

to STFdel (Figure 2C). These results indicate that the WUS box and STF box may act as partially redundant repression motifs and that their combined activity is required for full STF-mediated transcriptional repression.

The STFdel failure to complement *lam1* may be due to the loss of repressive activity. Consistent with this, fusion of the exogenous ethylene-responsive element binding factor–associated amphiphilic repression (EAR) motif repression domain SRDX to STFdel (*STF:SRDX-STFdel*) complemented *lam1* (Figure 2E), indicating that repressive activity is critical for STF function. To ascertain the individual contributions of the WUS box and STF box to STF function in planta, we performed *lam1* complementation by introducing mutant constructs (m1 and m2) individually or in combination under the control of the *STF* promoter (Figure 2D). Mutation in the WUS box, *STF:STFm1* (Lin et al., 2013), only partially complemented the *lam1* mutant, with plants showing wavy leaf margins (Figure 2F). Likewise, mutation in the STF box, *STF:STFm2*, partially complemented *lam1*, with even narrower leaf blades and more wavy margins compared with *STF:STFm1* transgenic plants (Figure 2G; Supplemental Table 1). The combined WUS box and STF box mutant (m1m2), on the other hand, completely failed to complement *lam1* (Figure 2H). Similar results were obtained for the complementation of the *M. truncatula stf* mutant by STFm1m2 (Supplemental Figure 2). These results demonstrate that the STF box and WUS box together account for the STF-repressive activity and are additively required for STF function in promoting leaf blade outgrowth.

The STF Box Is Conserved Only in Dicots and May Play a Stronger Role Than the WUS Box in Blade Outgrowth

To directly compare the ability of the WUS box and STF box in promoting leaf blade outgrowth, we fused either the WUS box or the STF box to STFdel driven by the *STF* promoter and introduced the constructs into *lam1* (Figure 3A). Both the *STF:STFdel-WUS-box* and *STF:STFdel-STF-box* constructs partially rescued *lam1* (Figures 3D and 3E), but the *STF:STFdel-STF-box* construct showed more complete rescue than did the *STF:STFdel-WUS-box* construct (Supplemental Table 1), suggesting that the STF box may be more important than the WUS box in promoting leaf blade outgrowth.

A BLAST search of sequenced genomes and ESTs revealed that the intact 10-amino acid STF box (QFIEFLPLKN) is conserved in dicots and the early-diverging angiosperm *Amborella trichopoda* but not in grasses, gymnosperms, or nonvascular plants. Amino acid alignment of the STF box in different dicot species showed that there is an LPL core motif, which is similar to the LQL core of the WUS box. However, unlike the WUS box LQL signature, the second Leu of the STF box LPL is not conserved in *Arabidopsis lyrata* WOX1 and *Mimulus guttatus* STL1 (Figure 3B). In *Aquilegia coerulea*, a eudicot phylogenetically located at the midpoint between grasses and core eudicots (Kramer, 2009), the STF-like1 (Aq STL1) protein sequence ends at the first Leu of the STF box (Figure 3B). This variability prompted us to test whether these two Leu residues have different significance for STF box function. We mutated either the first Leu (m2L1A) or the second Leu (m2L2A) to Ala in the presence of the m1 mutation and introduced the mutants into *lam1* plants (Figure 3C). Mutation of the first Leu (*STFm1-m2L1A*) completely abolished *lam1* complementation (Figure 3F), indicating that this amino acid is critical for STF box function. Mutation of the second Leu (*STFm1-m2L2A*), on the other hand, led to a small degree of rescue (Figure 3G), indicating that the second Leu of the STF box contributes to repressive function to a lesser extent than the first Leu. By contrast, both Leu residues in the LQL core sequence of the WUS box were conserved among WUS clade WOX genes, and mutation of either Leu of the WUS box in the presence of the m2 mutation (Figure 3C) completely abolished *lam1* complementation (Figures 3H and 3I), indicating that both Leu residues of the WUS box are equally important. From these observations, we concluded that the WUS box and STF box are repressive motifs additively required for STF-mediated leaf blade outgrowth, but the

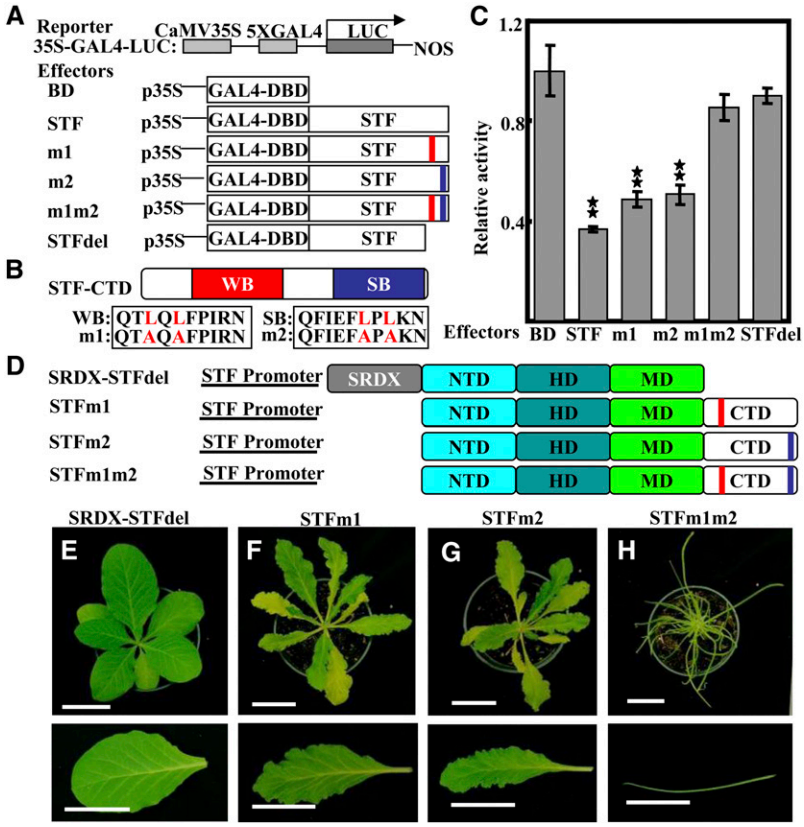

Figure 2. Both the WUS Box and STF Box in the CTD Are Required for STF Function.

(A) Schematic representation of reporter and effector constructs used in the luciferase assay. Red and blue lines represent the m1 and m2 mutations, respectively, shown in **(B)**.

(B) Leu (L) to Ala (A) substitution mutations in the CTD, yielding m1 in the WUS box (WB) and m2 in the STF box (SB).

(C) Relative luciferase activities using STF, STFm1, STFm2, STFm1m2, or STFdel as effector compared with the GAL4-DB control. Error bars indicate SD ($n = 3$). **P < 0.01 (*t* test).

(D) Constructs used for complementation of the *lam1* mutant. Red and blue lines represent m1 and m2 mutations, respectively.

(E) to **(H)** *lam1* mutant plants and leaves complemented with *STF:SRDX-STFdel* **(E)**, *STF:STFm1* **(F)**, *STF:STFm2* **(G)**, and *STF:STFm1m2* **(H)**. Bars = 5 cm.

dicot-specific STF box may play a slightly stronger role in this function.

STF Interacts with the Corepressor TPL via Its STF Box and WUS Box

To understand the molecular mechanisms underlying STF-mediated transcriptional repression in blade outgrowth, we performed yeast two-hybrid (Y2H) screening for STF partners using the Y2H Gold system. An *M. truncatula* protein with 83% amino acid identity to the *Arabidopsis* TPL protein was identified and designated Mt-TPL (Supplemental Figure 3). STF and Mt-TPL proteins interacted in Y2H assay under stringent conditions (Figure 4A). STF also interacted in Y2H with three of the four TPL-related proteins tested (Supplemental Figure 4). The interaction between STF and Mt-TPL was confirmed in planta by bimolecular fluorescence complementation (BiFC) assay using split YFP (Figure 4B; Supplemental Figure 5), while no YFP fluorescence was detected in negative controls where the split YFP was fused to either STF or Mt-TPL alone (Supplemental Figure 5). This interaction was further verified by a pull-down assay using plant-expressed protein (Szemenyei et al., 2008). Both maltose binding protein (MBP) and MBP-STF fusion protein were expressed in *Escherichia coli* and purified by binding to amylose resin. Equal amounts of MBP or MBP-STF proteins were immobilized by amylose resin, and the immobilized proteins were incubated with plant protein extract containing Mt-TPL-GFP fusion protein transiently expressed in tobacco (*Nicotiana benthamiana*) leaf cells. The MBP-STF fusion protein, but not the MBP control protein, was able to pull down the Mt-TPL-GFP fusion protein that was detected by anti-GFP antibody (Figure 4C), confirming the STF-MtTPL–specific interaction.

We next asked which domains of STF are responsible for this interaction and whether the Mt-TPL and STF interaction has biological relevance to leaf blade outgrowth. To answer these questions, we performed detailed Y2H assays combined with BiFC and transgenic analysis. STF deletion or substitution mutants were fused to GAL4-DBD and Mt-TPL was fused to

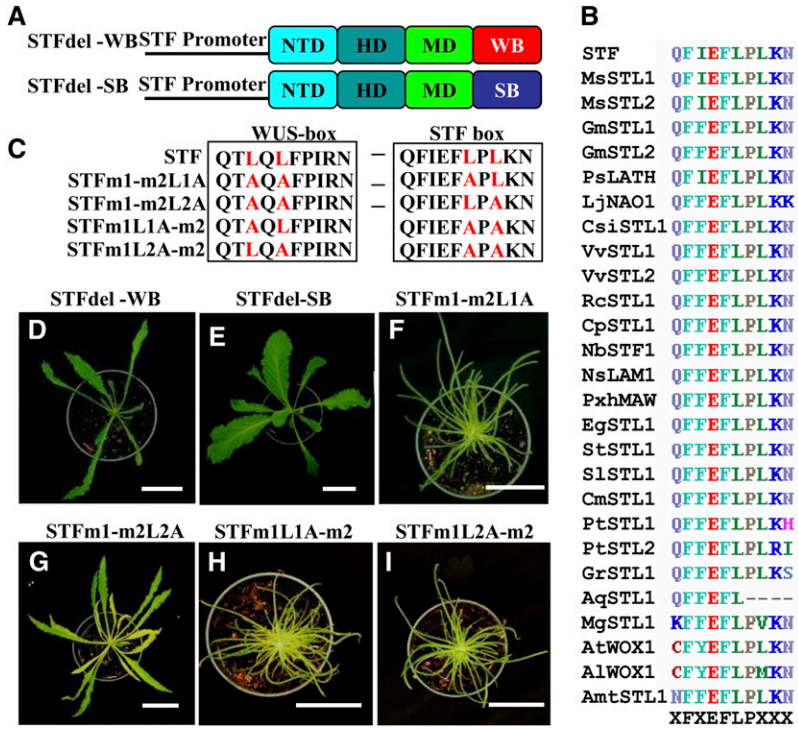

Figure 3. The STF Box Is Evolutionarily Conserved in Dicots and Plays a Stronger Role Than the WUS Box.

(A) Constructs used for complementation of the *lam1* mutants. Either WUS box (WB) or STF box (SB) was fused in-frame to the CTD-truncated mutant of STF (STFdel).

(B) Amino acid sequence alignment of the STF box in STF and STF-like (STL) proteins from dicot species. A consensus FxEFLP motif is shown at the bottom. Ms, *Medicago sativa*; Gm, *Glycine max*; Lj, *Lotus japonicus*; Csi, *Citrus sinensis*; Vv, *Vitis vinifera*; Rc, *Ricinus communis*; Cp, *Carica papaya*; Nb, *N. benthamiana*; Ns, *Nicotiana sylvestris*; Pxh, *Petunia* × *hybrida*; Eg, *Eucalyptus grandis*; St, *Solanum tuberosum*; Sl, *Solanum lycopersicum*; Cm, *Cucumis melo*; Gr, *Gossypium raimondii*; Aq, *Aquilegia coerulea;* Mg, *Mimulus guttatus*; At, *Arabidopsis*; Al, *Arabidopsis lyrata*; Amt, *Amborella trichopoda*.

(C) Leu (L) to Ala (A) mutations in STF box and WUS box.

(D) to **(I)** Phenotypes of transgenic *lam1* plants complemented with *STF:STFdel-WUS-box* **(D)**, *STF:STFdel-STF-box* **(E)**, *STF:STFm1-m2L1A* **(F)**, *STF:STFm1-m2L2A* **(G)**, *STF:STFm1L1A-m2* **(H)**, and *STF:STFm1L2A-m2* **(I)**. Bars = 5 cm.

GAL4-AD for Y2H analysis. Control assays were performed to confirm that these constructs did not show self-activation (Supplemental Figure 6). The interaction with Mt-TPL was completely abolished by deletion of the CTD (Figure 4D), indicating that the interaction with Mt-TPL is likely to be important for the STF-repressive activity. Whereas Mt-TPL was unable to interact with the CTD alone (Figure 4D), fusion of either the MD or HD to the CTD restored the interaction between the CTD and Mt-TPL (Figure 4D). This suggests that, while the STF CTD is essential for the interaction with Mt-TPL, additional sequences in the HD or MD may be required to stabilize this interaction.

Mutation of the two Leu residues in the WUS box somewhat reduced its interaction with Mt-TPL (Figure 4D), while this interaction was more strongly reduced by mutation of the STF box Leu residues (Figure 4D). Combined mutations in both the WUS box and STF box abolished the interaction with Mt-TPL (Figure 4D), consistent with the CTD deletion results. This finding was also verified by BiFC assay, in which the STFm1m2-YN coupled with TPL-YC failed to generate YFP signals (Figure 4E), demonstrating that both the STF box and WUS box functional motifs are required for the STF interaction with TPL. The interaction of the STFm1-m2L1A and STFm1-m2L2A mutants with TPL was also evaluated. Consistent with the complementation results (Figures 3F and 3G), the STFm1-m2L1A mutant showed no interaction with Mt-TPL (Figure 4D), while the STFm1-m2L2A mutant exhibited greatly reduced interaction (Figure 4D). Likewise, attachment of either the WUS box or STF box to the STFdel mutant restored limited interaction with TPL.

We also mapped the domains of Mt-TPL required for interaction with STF (Figure 4F). The N-terminal domain (amino acids 1 to 350; TPLdel), including the LiSH domain, CTLH domain, and Pro-rich domain (Szemenyei et al., 2008), was sufficient for interaction with STF (Figure 4G). Further truncation of part of the Pro-rich domain (amino acids 1 to 250; TPLdel2) showed no interaction with STF, suggesting that the Pro-rich domain is indispensable for interaction with STF. The *Arabidopsis tpl-1* mutant has a His substitution at Asn-176 (N176H), in the Pro-rich domain, which abolishes the interaction between TPL and AP2 (Krogan et al., 2012). We introduced an analogous mutation in Mt-TPL (TPL-m1). The m1 mutation abolished the

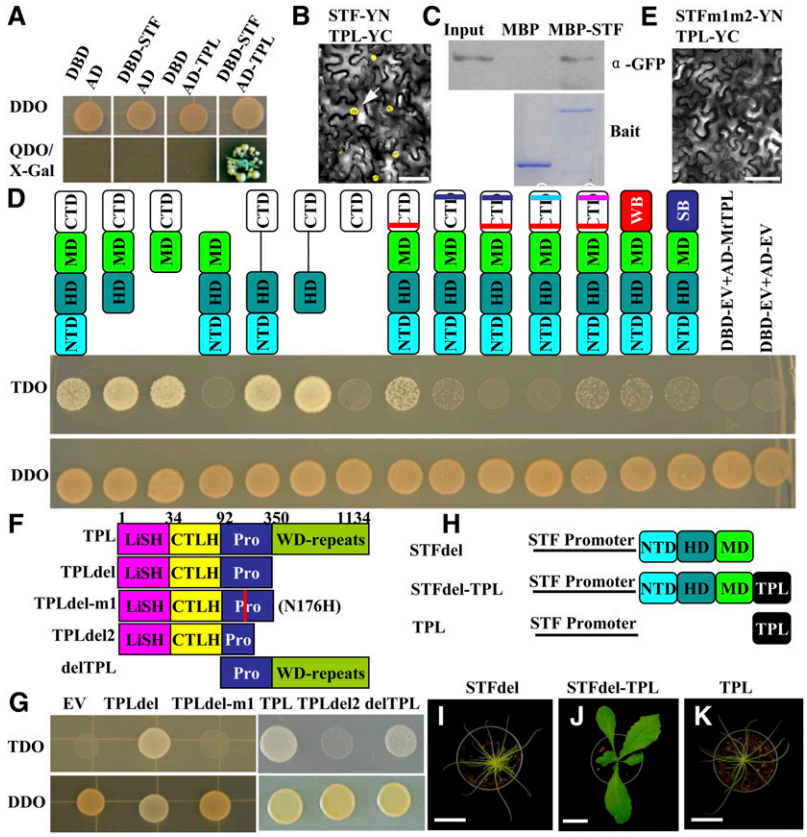

Figure 4. STF Physically Interacts with Mt-TPL through Its WUS Box and STF Box and This Interaction Is Required for Leaf Blade Outgrowth.

(A) Interaction between STF and Mt-TPL in the Y2H assay. Interaction was examined by the presence or absence of yeast growth on a quadruple dropout medium (QDO)/X-Gal plate. DDO, double dropout medium.

(B) Interaction between STF and Mt-TPL in living cells using a split YFP BiFC assay. Bar = 50 μm.

(C) Interaction between STF and Mt-TPL in pull-down assay. The TPL-GFP fusion protein, transiently expressed in tobacco leaves, was pulled down by amylose resin–immobilized MBP protein or MBP-STF fusion protein and detected by anti-GFP antibody (α-GFP). Immobilized MBP protein or MBP-STF fusion protein was stained by Coomassie blue and shown as bait.

(D) Mapping of the STF domains required for interaction with Mt-TPL. Different STF mutants were fused to the GAL4-DBD domain, while TPL was fused to the GAL4-AD domain. EV, empty vector. Interaction was examined by yeast growth on triple dropout medium (TDO). Data are representative of three repeats.

(E) BiFC showing the absence of interaction between STFm1m2 and TPL in living cells. Bar = 50 μm.

(F) Mapping of the Mt-TPL domains required for interaction with STF.

(G) Y2H interaction of the TPL mutant constructs in **(F)** with STF.

(H) Constructs used for complementation of *lam1* mutants.

(I) to **(K)** Phenotypes of *lam1* mutant plants complemented with *STF:STFdel* **(I)**, *STF:STFdel-TPL* **(J)**, and *STF:TPL* **(K)**. Bars = 5 cm.

interaction (Figure 4G). These data together suggested that the whole Pro-rich domain may be important for the TPL–STF interaction. Truncation of the LiSH and CTLH domains (amino acids 93 to 1134; delTPL) showed interaction with STF, but with greatly reduced strength (Figure 4G), suggesting that the LiSH and CTLH domains are not indispensable but may help in the TPL–STF interaction.

To provide direct evidence that STF and Mt-TPL interaction is essential for STF function, we constructed a chimeric fusion protein in which Mt-TPL was fused in-frame to the STFdel mutant, forming *STF:STFdel-TPL* (Figure 4H), and transformed it into *lam1* and *stf* mutants. Neither *STFdel* (Figure 4I) nor *TPL* (Figure 4K) alone rescued blade outgrowth in the mutant plants, but expression of the *STFdel-TPL* fusion complemented the mutant narrow leaf phenotypes with wavy margins (Figure 4J), demonstrating that the corepressor TPL is required for STF-mediated leaf blade outgrowth. This suggests that the primary function of the WUS box and STF box may be to recruit TPL to the STF repressor complex.

STF Represses *AS2* during Leaf Blade Development

The fact that STF acts as a transcriptional repressor and the HD is essential for its function indicates that STF may repress its target(s) involved in leaf development directly. In support of this notion, an Ile substitution at a conserved amino acid, Asn-147

(N147I; STFm3), in the third helix of the HD (Figure 5A), which is suggested to contact DNA (Zhang et al., 2010), abolished the ability of STF to complement the *lam1* mutant (Figure 5B).

In our previous genome-wide transcript profiling analysis of the *stf* mutant, several LOB domain proteins showed elevated expression (Tadege et al., 2011a). *AS2* encodes a LOB domain adaxial factor involved in leaf blade development in *Arabidopsis*. Since Mt-*AS2* was not represented by probes in the *M. truncatula* Affymetrix gene chip, we wondered whether Mt-*AS2* was upregulated in the *stf* mutant just like other LOB domain genes. We identified a single *AS2* homolog from the *M. truncatula* genome that showed 61% amino acid identity to *Arabidopsis* AS2 protein (Supplemental Figure 7A) and that complements the *Arabidopsis as2* mutant leaf phenotype and interacts with Mt-AS1 (Supplemental Figures 8A to 8C). Expression analysis by quantitative RT-PCR showed that Mt-*AS2* has 2-fold higher expression in the *stf* mutant and 5-fold lower expression in *STF*-overexpressing young leaves compared with wild-type leaves (Figure 5C), suggesting that *STF* may repress *AS2* expression. To evaluate this, we performed in situ hybridization in *M. truncatula* wild-type genotype R108 and *stf* mutant leaf primordia. In 4-week-old wild-type leaf primordium (P6 stage), *AS2* was expressed in the adaxial region but never reached the leaf margin or middle mesophyll, where *STF* was predominantly expressed (Figures 5D and 5G). In the *stf* mutant leaf primordium, *AS2* expression was extended to the leaf margin (Figures 5E and 5G), while the sense control showed no signal (Figure 5F), indicating that STF represses Mt-*AS2* activity at the leaf margin, where cell proliferation takes place.

We next examined whether STF directly binds to the Mt-*AS2* promoter and represses its activity. A 3-kb Mt-*AS2* promoter region immediately upstream of the translation start site was cloned and designated as *proAS2*. The *proAS2:AS2* construct, when introduced into the *Arabidopsis as2-1* mutant, rescued the asymmetric rosette leaf phenotype, suggesting that proAS2:AS2 is functional in transgenic *Arabidopsis* (Supplemental Figure 8A) and the 3-kb Mt-*AS2* upstream promoter region is sufficient to drive Mt-*AS2* function. We also transformed the *Arabidopsis wox1 prs* double mutant with the *proSTF:STF-YFP* construct, which fully rescued the narrow leaf phenotype (Supplemental Figure 8B), indicating that *STF-YFP* is also functional when introduced into *Arabidopsis*. To investigate if STF is able to bind the Mt-*AS2* promoter in plant cells, we performed chromatin immunoprecipitation (ChIP) assays using *Arabidopsis* leaf protoplasts from *proAS2:AS2/as2-1* transgenic lines, as described in Methods. PCR analysis revealed that several promoter fragments, P1, P2, P3, and P4, were enriched in the ChIP samples prepared with the anti-GFP antibody compared with the anti-HA antibody negative control (Figures 6A and 6B). By contrast, no PCR product was amplified using primers designed for the Mt-*AS2* coding region or the *Arabidopsis ACTIN* gene, indicating that these sequences were absent from the immunoprecipitated chromatin (Figure 6B). Taken together, the ChIP assay indicates that STF specifically binds the Mt-*AS2* upstream promoter region in vivo.

To test whether STF protein can directly bind to the fragments recovered by the ChIP assays, we performed electrophoretic mobility shift assay (EMSA). The P2 and P3 fragments were amplified by PCR and then labeled by biotin at the 3′ end, while the unlabeled probes were used as competitors. EMSA results showed that the recombinant MBP-STF protein was able to bind

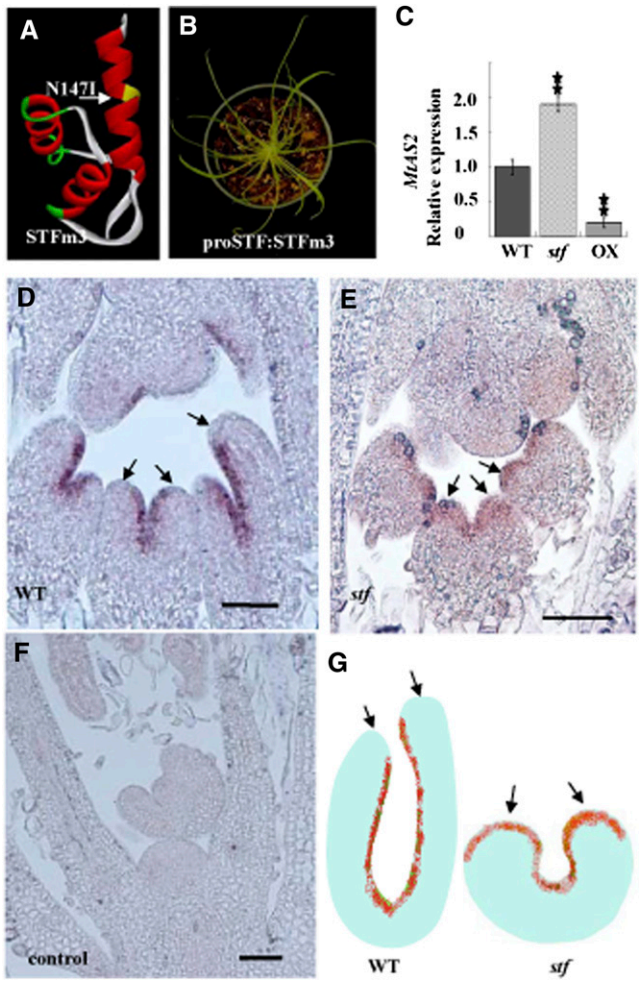

Figure 5. STF Represses *AS2* Expression at the Leaf Margin in *M. truncatula*.

(A) Structure of the STF HD based on template 2da3A. A point mutation (m3, Asn to Ile) in position 147 is shown.

(B) *N. sylvestris lam1* mutant complemented with mutated Mt-STFm3. The N147I mutation abolished the STF activity in complementing the *lam1* mutant.

(C) Relative expression level of *AS2* in the *M. truncatula* wild type, *stf* mutant, and *STF* overexpression lines (OX). The expression level of *AS2* in the wild type was set to 1.0. Error bars indicate SD (n = 3). **P < 0.01 (t test, compared with the wild type).

(D) to **(F)** RNA in situ hybridization showing Mt-*AS2* expression viewed in longitudinal sections of 4-week-old shoot apices in the wild type **(D)** and the *stf* mutant **(E)**. A negative control is shown in **(F)** using sense probe. Arrows in **(D)** and **(E)** indicate the absence or presence of *AS2* signal at the leaf margin in wild-type and *stf* mutant leaf primordia, respectively. Bars = 50 μm.

(G) A cartoon depicting the expression pattern of *AS2* (red) in wild-type and *stf* mutant leaf primordia observed in **(D)** and **(E)**. Note that *AS2* expression is excluded from the leaf margin in the wild type, while expression is extended beyond the margin into the abaxial domain in the *stf* mutant.

to P2 and P3 fragments, while binding was not detected by the control MBP protein (Figures 6C and 6D). Furthermore, 50-fold excess unlabeled probes competed out the binding completely (P2 fragment) or mostly (P3 fragment). We also detected binding between STF protein and the P4 fragment (Figure 6F). The STF

m3 mutation in the HD, as expected, abolished the STF–DNA interaction for P2, P3, or P4 (Figures 6E and 6F). These biochemical data together indicate that STF protein can directly bind to multiple sites in the *AS2* promoter.

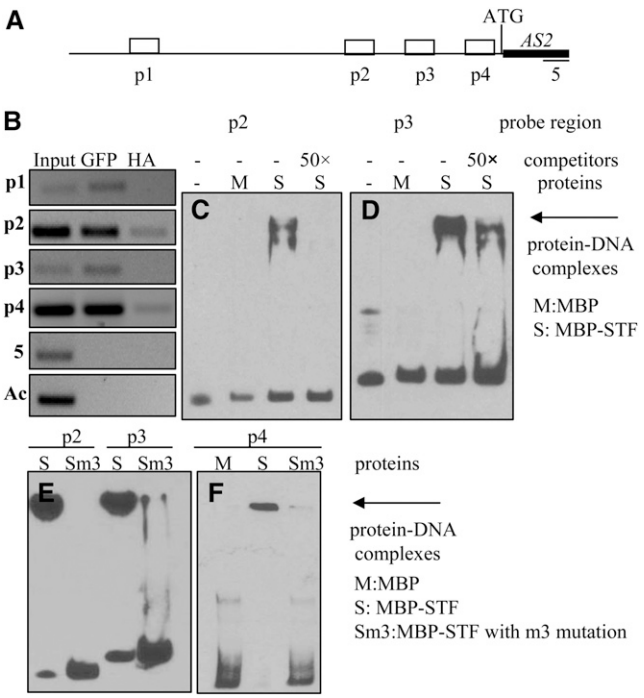

Figure 6. STF Directly Binds to the Mt-*AS2* Upstream Promoter Region.

(A) Schematic representation of the *proAS2:AS2* construct, which complemented the *Arabidopsis as2-1* asymmetric leaf phenotype. The promoter regions tested by ChIP assays are indicated as P1, P2, P3, and P4. The Mt-*AS2* coding region (from the translation start site ATG) is shown by the thick line, and the CDS region tested by the ChIP assay is designated as 5.

(B) ChIP assays. The *proAS2:AS2/as2-1* leaf protoplasts were transfected by pro35S:STF-YFP. Chromatin complexes were cross-linked by formaldehyde, fractioned by sonication, immunoprecipitated by anti-GFP antibody or anti-HA antibody, and collected by protein A agarose beads. The purified DNAs were used as templates for PCR. PCR products for P1, P2, P3, and P4 were enriched in anti-GFP samples compared with the anti-HA samples. For the Mt-*AS2* coding region (5) and the *Arabidopsis ACTIN* gene (Ac), no PCR products were detected. Similar results were obtained from three biological replicates.

(C) EMSA showing MBP-STF (S) bound to the biotin-labeled P2 promoter fragment but not to the MBP (M) control. Fifty times (50×) unlabeled P2 DNA completely competed out the binding (right lane).

(D) EMSA showing MBP-STF (S) bound to the biotin-labeled P3 promoter fragment but not to the MBP (M) control. Fifty times (50×) unlabeled P3 DNA competed out this binding to a large extent.

(E) Compared with the MBP-STF fusion protein (S), which bound to the P2 and P3 promoter fragments, the MBP-STFm3 fusion protein (Sm3) lost the ability to bind DNA, confirming that the Asn-147 site of the HD is critical for STF interaction with the *AS2* promoter.

(F) EMSA showing MBP-STF (S) bound to the biotin-labeled P4 promoter fragment but not to the MBP (M) control or the m3 mutant (Sm3).

To further establish that STF can repress Mt-*AS2* promoter activity in protoplasts, a dual luciferase assay was performed in *Arabidopsis* protoplasts. The 3-kb Mt-*AS2* upstream promoter region was fused to mini 35S driving the luciferase reporter gene (Figure 7A). The addition of STF effector significantly repressed Mt-*AS2* promoter activity compared with the GUS control, while STFdel or STFm3 failed to repress it (Figure 7B). This result indicates that both the HD and CTD are required for STF-mediated repression of Mt-*AS2*.

The CTD of STF is required for interaction with Mt-TPL as well as for STF repression of Mt-*AS2*, suggesting that the STF-MtTPL complex may be involved in the repression of Mt-*AS2*. Since Mt-STF had repressive activity in *Arabidopsis* protoplasts, we hypothesized that in the *Arabidopsis tpl-1* background, Mt-STF would not fully repress the transcription of Mt-*AS2* if TPL is required for this repression. To test this hypothesis, we performed a dual luciferase assay in *Arabidopsis tpl-1* mutant protoplasts using STF as effector. In Landsberg *erecta* (L*er*) protoplasts, luciferase relative activity was reduced by more than half in the presence of the STF effector compared with the GUS effector control (Figure 7C). However, in the *Arabidopsis tpl-1* mutant protoplasts, STF lost its repression activity and no significant difference was observed between GUS and STF effectors (Figure 7C), indicating that the STF repression of Mt-*AS2* promoter activity requires the TPL protein.

As shown in Figure 4, the STFdel-TPL fusion is able to rescue the *N. sylvestris lam1* leaf blade phenotype. To check if the STFdel-TPL fusion can repress Mt-*AS2* expression in planta, we introduced STFdel and STFdel-TPL fusion constructs under the control of the *STF* promoter into the *M. truncatula stf* mutant. In agreement with the *lam1* complementation, STFdel showed no sign of complementation, while the STFdel-TPL fusion showed partial rescue of the *stf* mutant leaf blade with enhanced margin serrations (Figure 7D). We then compared the expression of Mt-*AS2* transcript by real-time PCR in these transgenic lines. Consistent with the transgenic phenotypes, in the STFdel-transformed *stf* mutant plants, Mt-*AS2* expression was elevated by approximately 2-fold over the wild type, similar to the untransformed *stf* mutant, while in the *STF*-complemented *stf* mutant, the Mt-*AS2* expression level was similar to that in the wild type (Figure 7E). Interestingly, the *STFdel-TPL* fusion–complemented lines showed reduced Mt-*AS2* expression comparable to the *STF*-complemented lines (Figure 7E), indicating that the STF-TPL repressor complex represses Mt-*AS2* in planta. Taken together, these data indicate that recruitment of the corepressor TPL by the CTD of STF is required for direct repression of *AS2* at the leaf margin during leaf blade development.

Silencing of Mt-*AS2* Promotes Leaf Blade Outgrowth, While Overexpression of Mt-*AS2* in *N. sylvestris* Results in a Narrow Leaf Phenotype

To investigate the role of *AS2* in *M. truncatula* leaf development, we generated *AS2*-downregulated *M. truncatula* plants via RNA interference (RNAi). Silencing of Mt-*AS2* in the wild type or in the *stf* mutant caused epinastic leaves (Figure 8A; Supplemental Figure 9A). Silencing of *AS2* in the wild type resulted in wider leaf blades (Figure 8A), while silencing of *AS2* in the *stf* mutant partially rescued the narrow leaf blade and smooth leaf margin phenotypes of *stf* (Figure 8B; Supplemental Figure 9B), suggesting that ectopic expression of *AS2* partly

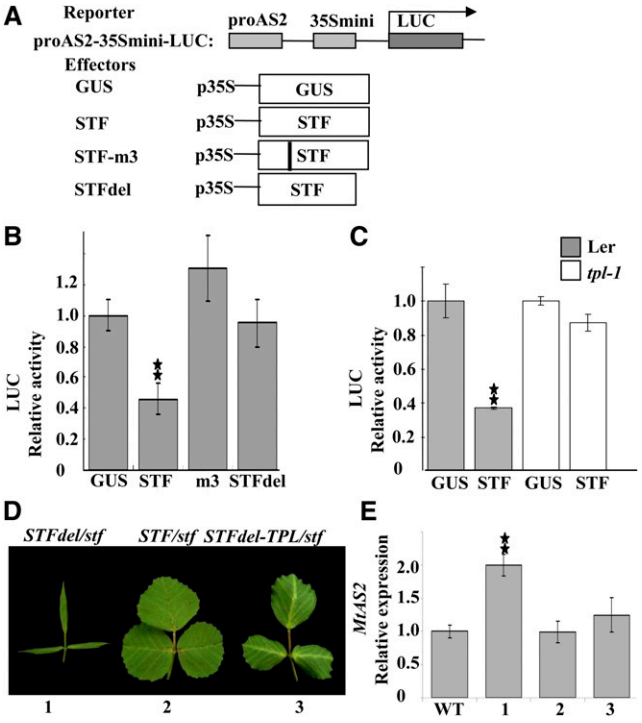

Figure 7. The STF-TPL Complex Represses Mt-*AS2* Promoter Activity.

(A) Schematic representation of reporter and effector constructs used in the luciferase assay. The 3-kb Mt-*AS2* promoter region was fused to a mini 35S promoter to drive the expression of the luciferase reporter gene. Elements of the scheme are not drawn to scale.

(B) Relative luciferase activities in *Arabidopsis* protoplasts using STF, STFm3, or STFdel as effector compared with the GUS control. Error bars indicate SD ($n = 3$). **P < 0.01 (*t* test).

(C) Relative luciferase activities using Mt-STF as effector compared with the GUS control in *Arabidopsis* wild-type (L*er*) or *tpl-1* mutant protoplasts. Error bars indicate SD ($n = 3$). **P < 0.01 (*t* test).

(D) Complementation of *M. truncatula stf* mutant leaf blade phenotypes by *STF:STFdel* (1), *STF:STF* (2), and *STF:STFdel-TPL* (3) constructs.

(E) Relative expression of *AS2* determined by quantitative RT-PCR in the *stf* mutant background complemented with *STFdel* (1), *STF:STF* (2), and *STF:STFdel-TPL* (3) compared with the wild type. The expression level of *AS2* in the wild type was set to 1.0. Error bars indicate SD ($n = 3$). **P < 0.01 (*t* test).

[See online article for color version of this figure.]

accounts for the narrow blade phenotype of the *stf* mutant. To further evaluate the consequences of Mt-*AS2* ectopic expression, we transformed Mt-*AS2* under the control of the cauliflower mosaic virus *35S* promoter into *N. sylvestris* wild-type and *lam1* mutant plants. Compared with the broad and flat wild-type leaves (Figure 8C), the Mt-*AS2*–overexpressing plants showed a range of blade phenotypes from severe curling to needle-like leaves (Figures 8D to 8F; Supplemental Figure 10). Likewise, overexpression of Mt-*AS2* in the *lam1* background worsened the *lam1* mutant phenotype, producing shorter and erect leaves (Figure 8G). These data collectively indicate that *STF*-mediated repression of *AS2* is essential for proper leaf blade development.

DISCUSSION

The WUS Box and STF Box of STF Are Repressive Motifs and Cooperatively Recruit the Corepressor TPL

WUS clade *WOX* genes are essential players in several plant developmental programs, including stem cell maintenance, embryonic patterning, seed development, leaf development, and flower development (Schoof et al., 2000; Lohmann et al., 2001; Matsumoto and Okada, 2001; Nardmann et al., 2004; Sarkar et al., 2007; Breuninger et al., 2008; Shimizu et al., 2009; Vandenbussche et al., 2009; Ji et al., 2010; Tadege et al., 2011a; Nakata et al., 2012). A common mechanism of action in WUS clade *WOX* genes is their ability to act as transcriptional repressors (Lin et al., 2013). Here, molecular dissection of the *M. truncatula* WUS clade protein STF into four domains, NTD, HD, MD, and CTD, enabled us to gain mechanistic insight into the complexity of this repression mechanism. Our work underlines that DNA binding ability, mediated by the HD, and recruitment of corepressors, mediated by the CTD motifs, are critical for STF function. A single amino acid substitution in the HD (m3) abolished both the DNA binding ability and biological function. Thus, direct contact with DNA is indispensable for STF to promote leaf blade outgrowth. We demonstrated that two conserved motifs at the CTD, the WUS box and the STF box, are additively required for mediating transcriptional repression. These two motifs cooperate to recruit the TPL family corepressors into the STF repressor complex, and this recruitment is essential for leaf blade morphogenesis. The requirement for both the WUS box and STF box to complement the *lam1* mutant can be bypassed by directly fusing Mt-TPL to truncated STF lacking these two motifs (Figure 4J), indicating that TPL is an essential partner of STF in the regulation of leaf blade development. These observations are in agreement with previous reports from *Arabidopsis*, in which the WUS box was shown to be required for WUS-repressive activity (Kieffer et al., 2006; Ikeda et al., 2009a) and TPL was shown to interact with the EAR-like motif (Szemenyei et al., 2008; Causier et al., 2012; Krogan et al., 2012; Wang et al., 2013), which closely resembles the WUS box and the STF box.

The STF Box Is Specific to Dicots

The WUS box and STF box appear to have been acquired relatively late in the evolution of *WOX* genes, with the WUS box preceding the STF box. The intact WUS box is conserved in the WUS clade (WUS, WOX1 to WOX7) WOX members found in seed plants, while partial sequences of WUS box sequences exist in intermediate and ancient WOX clades found in earlier diverging taxa (Lin et al., 2013). The intact STF box, on the other hand, is detected so far only in nonmonocot angiosperms, including the early-diverging angiosperm *A. trichopoda* (Figure 3B). *A. trichopoda* is a fascinating plant from an evolutionary standpoint, as it is the only extant species of the family Amborellaceae (endemic to the island of New Caledonia), having diverged from the angiosperm lineage 130 million years ago (Soltis et al., 2008). Interestingly, the vesselless *A. trichopoda* has a typical dicot leaf blade with reticulate venation. One possibility is that *A. trichopoda*, along with eudicots but not grasses, acquired the *STF* lineage with its

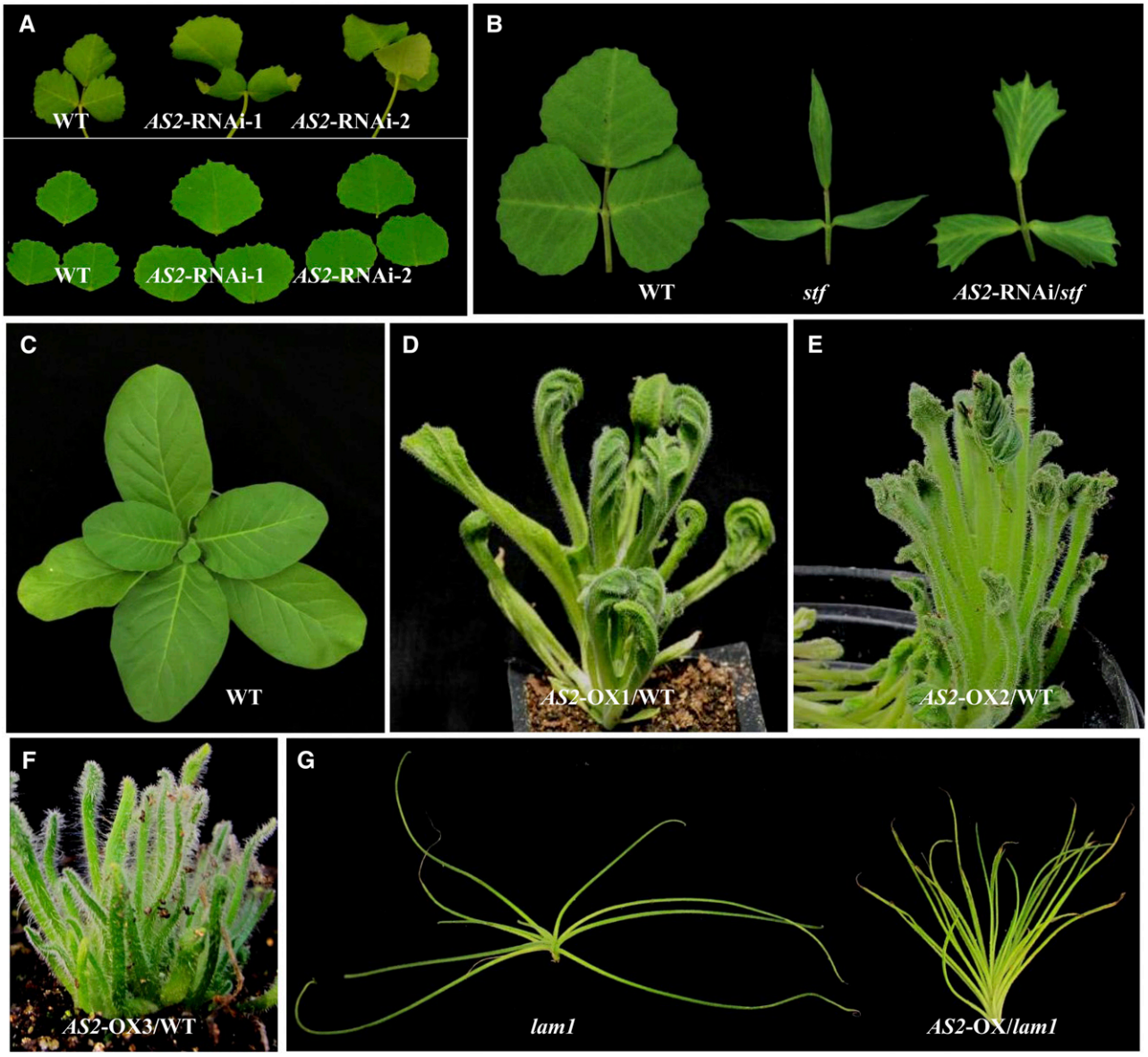

Figure 8. Silencing of *AS2* by RNAi in *M. truncatula* and Overexpression of Mt-*AS2* in *N. sylvestris*.

(A) Silencing of *AS2* in wild-type *M. truncatula* leaves caused epinastic (top panel) and bigger (bottom panel) blades. Leaves of two representative RNAi lines are shown.
(B) Silencing of *AS2* in the *M. truncatula stf* mutant led to partial complementation of the leaf blade phenotype (right) compared with the mutant (middle) and the wild type (left).
(C) Wild-type *N. sylvestris* control plant.
(D) to **(F)** Phenotypes of *N. sylvestris* transgenic lines expressing the *35S:AS2* transgene showing severe upward curling and needle-like blades. Three representative transgenic lines are shown.
(G) Untransformed *N. sylvestris lam1* mutant (left) and *lam1* mutant transformed with the *35S:AS2* transgene showing shorter and more erect leaves than *lam1* (right).
[See online article for color version of this figure.]

characteristic STF box. Another possibility is that the specialized grass leaves may have lost the STF box during evolution. Further research using fossils and extant plants will help test these hypotheses and shed light on the evolution of angiosperm leaf development.

The WOX-TPL Repressor Complex May Have a Widely Conserved Function in Cell Proliferation

WUS acts as a transcriptional repressor in stem cell maintenance in the shoot apical meristem in *Arabidopsis* (Kieffer et al., 2006;

Ikeda et al., 2009a). WUS has a WUS box and an EAR-like motif at its C terminus, both of which are required for its repressive activity (Kieffer et al., 2006; Ikeda et al., 2009a). Interestingly, WUS also interacts with TPL via the WUS box, and this interaction is important for WUS function in floral organ development (Causier et al., 2012). However, WUS acts as an activator of *AGAMOUS* expression in the flower (Lohmann et al., 2001; Ikeda et al., 2009a), and whether TPL is required for WUS function in vegetative meristem stem cell maintenance has yet to be determined. Fusion of TPL to a mutated WUS protein (WUSΔ) that lacks the WUS box and EAR motif partially rescues the inflorescence and flower meristems but fails to rescue the vegetative meristem phenotypes of the *wus-1* mutant (Causier et al., 2012). Based on such observations, Causier et al. (2012) suggested that TPL may not be required for WUS function in vegetative tissues of *Arabidopsis*. Our experiments, showing complementation of the *lam1* mutant with STFdel-TPL fusion and a lack of Mt-STF–repressive activity in the *Arabidopsis tpl-1* mutant, clearly demonstrated that TPL is required for STF function, a WUS-like cell proliferative function at the leaf margin that can be substituted by *Arabidopsis* WUS in tobacco *lam1* and *M. truncatula stf* mutants (Tadege et al., 2011a; Lin et al., 2013). TPL interacts with a wide range of WUS clade WOX proteins, including WOX2, WOX4, and WOX5, and potentially all WUS clade members (Causier et al., 2012), suggesting that the interaction of TPL with the WUS clade members may be a conserved common mechanism that forms repressor complexes involved in regulating key plant developmental programs, including embryo patterning, stem cell maintenance, and lateral organ development.

The STF-TPL Complex Represses *AS2* at the Adaxial-Abaxial Junction of the Leaf Margin

The development of plant lateral organs requires the coordination of cell division and cell differentiation. The major defect of the *stf* mutant leaf is a drastic reduction in leaf cell number in the lateral direction, which accounts for most of the narrow blade phenotype (Tadege et al., 2011a, 2011b). *STF* is expressed in a narrow domain at the adaxial-abaxial junction of leaf primordia including both the leaf margin and the middle mesophyll (Tadege et al., 2011a). We identified Mt-*AS2* as a direct target of STF based on several types of experimental evidence, including ChIP, EMSA, luciferase assay, and expression analysis. In the ChIP analysis, STF associated with several regions in the Mt-*AS2* promoter, indicating that STF may bind multiple sites in the *AS2* promoter. This is similar to the direct regulation of *ARR7* by WUS in *Arabidopsis*, which was found to be associated with 11 regions spreading over the 2-kb *ARR7* promoter in the ChIP assay (Leibfried et al., 2005). The identification of Mt-*AS2* as one of the *STF* direct targets explains some of the observed leaf blade phenotypes of the *stf* mutant. In *Arabidopsis*, AS2 is an adaxial polarity factor that, together with AS1, promotes cell differentiation and adaxial identity. The expression of *AS2* is repressed directly by KANADI (KAN) in the abaxial domain. A G-to-A mutation in the KAN binding sites results in ectopic expression of *AS2* in the abaxial domain and leads to adaxialized leaves of relatively normal size (Wu et al., 2008). It is possible that *AS2* expression is still excluded from the *WOX1/PRS* region because of the repression activity of WOX1/PRS, and cell proliferation may not be affected substantially. Consistent with this, the *wox1 prs kan1 kan2* quadruple mutant shows a very narrow leaf blade (Nakata et al., 2012). In *M. truncatula*, *AS2* expression is restricted to the adaxial domain of the leaf primordium and is excluded from the *STF* expression domains in the leaf margin and middle mesophyll. In the *stf* mutant, the *AS2* expression domain is expanded to the leaf margin (Figure 5), suggesting that it could repress cell proliferation at the margin by promoting premature differentiation of margin cells. In support of this, we found that silencing of *M. truncatula AS2* broadens the leaf blade and partially complements the *stf* mutant, while its ectopic expression in *N. sylvestris* severely compromises leaf blade outgrowth (Figure 8). It is likely that STF coordinates cell proliferation, at least in part, by preventing the expression of cell differentiation polarity factors, including *AS2*, in the MD. Whether *STF* also directly represses abaxial polarity factors such as *KAN*, *YABBY*, *ARF3*, and *ARF4*, and whether this repression accounts for additional *stf* mutant phenotypes, remain to be shown. *STF/LAM1* could establish and maintain a cell proliferation zone in the MD by repressing polarity factors, which may enable the achievement of a balance between cell proliferation and differentiation during leaf blade development. The requirement of Mt-*TPL* for both the repression of Mt-*AS2* by *STF* and the *STF*-mediated regulation of blade outgrowth indicates that transcriptional repression of *AS2* by the STF-TPL complex is essential for leaf blade development.

Taken together, our findings shed light on the mechanism of *STF*-mediated regulation of leaf blade outgrowth and suggest that the WOX-TPL complex may modulate crucial functions in plant development.

METHODS

Plant Materials and Growth Conditions

The *Medicago truncatula* genotype R108 and *stf* mutant, *Nicotiana sylvestris* wild type and *lam1* mutant, and *Arabidopsis thaliana* ecotype L*er* and *tpl-1* mutant (Long et al., 2006) as well as Columbia and *wox1 prs* double mutant (Vandenbussche et al., 2009) were used in this research. Plants were grown at 24°C/16-h (day) and 20°C/8-h (night) photoperiods, 70 to 80% relative humidity, and 150 μmol m^{-2} s^{-1} light intensity in a greenhouse or growth chambers.

Sequence Alignment and Phylogenic Analysis

Alignment of the amino acid sequences was performed using BioEdit software and the ClustalW program (http://bioedit.software.informer.com/). Phylogenic analysis was performed using MEGA5.2 (neighbor-joining method using default settings with 1000 bootstrap replications; http://www.megasoftware.net/). The alignment used to generate the tree is available as Supplemental Data Set 1.

Plasmid Construction and Plant Transformation

All the primers used in this study are listed in Supplemental Table 2. All *lam1* or *stf* complementation assays utilize the pSTF-pMDC32 Gateway vector, in which the 2× 35S promoter in pMDC32 was replaced by the *STF* promoter as described (Lin et al., 2013). The deletion mutations in *STF* (HD-MD-CTD, NTD-HD-CTD, HD-CTD, MD-CTD, and STFdel) were constructed using appropriate primers. The mutations in *STF* (*STFm1*, *STFm2*, *STFm3*, *STFm1-m2L1A*, *STFm1-m2L2A*, *STFm1L1A-m2*, *STFm1L2A-m2*, and *STFm1m2*) and *TPLm1* were introduced using appropriate mutagenic primers; *SRDX-STFdel* was

constructed using synthetic sense primers with SRDX sequence. Fusion of WUS box or STF box to the *STFdel* mutant was performed using synthetic reverse primers containing either WUS box or STF box. To make the STFdel-TPL fusion protein, *STFdel* without a stop codon was cloned into the *Sal*I and *Eco*RI sites of pRS300 vector (Schwab et al., 2006). Mt-*TPL* was then cloned in the *Eco*RI and *Not*I sites of pRS300-STFdel. *STF* forward primer and *TPL* reverse primer were used to amplify the *STFdel-TPL* fusion gene from pRS300-STFdel-TPL. All regions corresponding to the transgene were cloned into the pSTF-pMDC32 vector by using the Gateway system (Invitrogen). For Mt-*AS2* constructs, the Mt-*AS2* coding region (with or without stop codon) was amplified and cloned into pDONR207 vector and was transferred by LR reaction to other plasmids, including pMDC32 (overexpression) and pK7GWIWG2D(II) (for RNAi).

Constructs were introduced into *Agrobacterium tumefaciens* by freeze shock. *Agrobacterium* strain GV2260 was used for *N. sylvestris* transformation, strain GV3101 was used for *Arabidopsis* transformation, and strain AGL1 was used for *M. truncatula* transformation as described (Tadege et al., 2011a). Transgenic plants were first confirmed by PCR genotyping, and at least three independent transgenic plants were further confirmed by RT-PCR to ensure that the constructs were expressed properly. The phenotypes of *lam1* complementation by different STF mutant proteins are listed in Supplemental Table 1.

Transient Expression Assays

Construction of the reporter GAL4-LUC plasmid was described previously (Ikeda et al., 2009a). For effector plasmids, the coding sequences of *STF* and mutant derivatives of *STF* (*STFm1*, *STFm2*, *STFm1m2*, and *STFdel*) were first cloned into pGBKT7. Then, the coding regions of the BD fusion were amplified using appropriate primers and cloned into p2GW7 using the Gateway system (Invitrogen) to yield effector plasmids.

Construction of the reporter proAS2-mini-35S-LUC plasmid was conducted as follows. First, a mini 35S promoter (Lodha et al., 2013) was synthesized and annealed. Second, PCR was performed with proMtAS2-F and proMtAS2-R-35S primers, which amplified the 3-kb Mt-*AS2* promoter region with a mini 35S extension. Third, the PCR product was mixed with the annealed 35S promoter and used as the template to clone the proAS2-35S-mini fusion, which was cloned into pCR8-D-TOPO vector and recombined with p2GWL7 using LR reaction to yield the reporter.

Transient expression assays were performed with *Arabidopsis* protoplasts as described (Asai et al., 2002). For each transformation, 5 μg of reporter plasmid and 4 μg of effector plasmid were used. For normalization of the activity of the reporter gene, 0.5 μg of plasmid pRLC was used as an internal control.

Y2H Library Construction and Screening

An *M. truncatula* whole-plant Y2H library was prepared in the pGADT7-Rec plasmid (prey) and transformed into yeast strain Y187 (Clontech; Make Your Own "Mate and Plate" Library System). Full-length *STF* coding sequence was cloned into the *Eco*RI and *Bam*HI sites of bait vector pGBKT7, which was transformed to yeast strain Y2H Gold (Clontech). Library screens were performed by yeast mating between the bait and prey strains according to the manufacturer's instructions (Clontech; Matchmaker Gold Yeast Two-Hybrid System User Manual). Over 1 million diploids were screened for interactions, and putative positives were isolated on minimal medium plates lacking His but containing 100 ng/mL aureobasidin A (for reporter *AUR1-C*). Interactions were further validated by the use of the *ADE2* (−ade) and/or *MEL1* (X-α-Gal) reporters. Positive interactor plasmids were isolated using the Easy Yeast Plasmid Isolation kit (Clontech), and each plasmid was individually retransformed into Y2H Gold with pGBKT7-STF for further confirmation. Plasmids that were confirmed to be positive with all the reporters (*AUR1-C*, *HIS3*, *ADE2*, and *MEL1*) were sequenced.

ChIP Assays

The ChIP assays were performed as described previously (Lee et al., 2007; Du et al., 2009; Xiong et al., 2013). Two million protoplasts from 14-d-old *proMtAS2:MtAS2/as2-1* transgenic plant leaves were transformed with 60 μg of pro35S:STF-YFP DNA using the polyethylene glycol–mediated transformation method. Protoplasts were incubated at room temperature for 12 h under dark conditions. Protoplasts were cross-linked by 1% formaldehyde in W5 medium for 20 min and quenched with Gly (0.2 M) for 5 min. The protoplasts were then lysed, and the DNA was sheared on ice with sonication. The sheared chromatin was precleared by salmon sperm–sheared DNA/protein A agarose beads. Precleared chromatin (100 μL) was kept as input, while the remaining supernatant was divided into two equal volumes (1.4 mL each), with 5 μL of anti-GFP antibody (ab290) added to one and 5 μL of anti-HA antibody (ab9110) added to the other. After overnight incubation at 4°C, protein A agarose beads (40 μL) were added to each, and the samples were incubated at 4°C for 2 h to collect the immunoprecipitate. Beads were then washed five times, resuspended in elution buffer, and incubated at 65°C overnight to reverse the cross-link. DNA was purified and diluted 2-fold, and 2 μL of DNA was used as a template for each PCR amplification. The input DNA and HA antibody–precipitated DNA were used as PCR templates for the positive and negative controls, respectively. The PCR products were visualized after 35 cycles. Experiments were repeated three times with similar results. The primers used for the ChIP assays are described in Supplemental Table 2.

EMSA

The Mt-*AS2* promoter fragments (P2 to P4) were amplified by PCR using Fusion *Taq* and labeled by using the Biotin 3′ End DNA Labeling kit (Pierce) according to the manufacturer's manual. Fifty times molar unlabeled probes were used as competitors in the competing assays. Purified MBP, MBP-STF, and MBP-STFm3 were used in the EMSA. EMSA was performed as described previously (Zhang et al., 2010).

Pull-Down Assays

Full-length *STF* CDS was amplified with appropriate primers, cloned to the *Nco*I and *Hin*dIII sites in pMBP-28b vector, and introduced to *Escherichia coli* BL21 (DE3) cells for expression. The expression of MBP-STF fusion protein was induced by 0.1 M isopropyl β-D-1-thiogalactopyranoside at 24°C for 9 h and purified using the amylose resin (New England Biolabs). Purified proteins were dialyzed with 1× PBS buffer with 10% (v/v) glycerol and quantified by Bradford kit (Bio-Rad). Equal amounts of MBP-STF or MBP proteins were immobilized to amylose resin beads. An aliquot of 50 μL of MBP-STF beads or MBP beads was boiled in 50 μL of Laemmli buffer (4% SDS, 20% glycerol, 0.02% bromophenol blue, 10% β-mercaptoethanol, and 125 mM Tris-HCl, pH 6.8). Ten microliters of supernatant was loaded onto an SDS-PAGE gel, stained with Coomassie Brilliant Blue R 250, and used as the bait control. Plant lysates were prepared from infiltrated tobacco (*Nicotiana benthamiana*) leaves using lysis buffer (50 mM PBS, 150 mM NaCl, 1% Triton X-100, 15% glycerol, and proteinase inhibitor cocktail 1:100 from Sigma-Aldrich). An aliquot of 1.2 mL of lysates was first precleared by incubating with 100 μL of amylose resin for 1 h. An aliquot of 0.5 mL of precleared lysate was incubated with 50 μL of MBP-STF beads or MBP beads for 2.5 h. The MBP-STF beads or MBP beads were centrifuged and washed five times with wash buffer (50 mM PBS, 150 mM NaCl, 1% Triton X-100, 10% glycerol, and proteinase inhibitor cocktail 1:100). After the final wash, beads were boiled in 50 μL of Laemmli buffer. Immunoblot analysis was performed using rabbit anti-GFP primary antibody (1:5000; Abcam) and goat anti-rabbit IgG secondary antibody (1:10,000; Abcam).

Y2H Assays

The bait and prey clones used in Y2H assays were cloned into the Gateway version of pGBKT7-GW (bait) and pGADT7-GW (prey) vectors

using the recombination-based Gateway cloning system (Invitrogen). Sets of constructs were cotransformed into Y2H Gold yeast strain (Clontech). Yeast transformants were selected on synthetic minimal double dropout medium deficient in Trp and Leu. Protein interaction tests were assessed on triple dropout medium deficient in His, Trp, and Leu or quadruple dropout medium deficient in His, Trp, Leu, and adenine with X-α-Gal. At least three clones were analyzed, and experiments were repeated three times with similar results.

BiFC Analysis and Confocal Microscopy

BiFC assays were conducted according to Lu et al. (2010). Briefly, *STF*, *STFm1m2*, and Mt-*AS1* were cloned into pEARLEYGATE201-YN, while Mt-*TPL* and Mt-*AS2* were cloned into pEARLEYGATE202-YC, by LR reaction. *STF-YN*, *STFm1m2-YN*, *AS1-YN*, *TPL-YC*, and *AS2-YC* were introduced into *Agrobacterium* by freeze shock. Pairs of combinations were coinfiltrated into 4-week-old *N. benthamiana* leaves. P19 was used to inhibit transgenic silencing. YFP signal was observed 48 to 60 h after infiltration by a TCS SP2 AOBS confocal laser scanning microscope (Leica Microsystems). Results were verified in at least three repeats.

In Situ Hybridization

RNA in situ hybridization was performed on shoot apices of 4-week-old *M. truncatula* plants using *AS2*-specific probe. An Mt-*AS2*–specific fragment of 319 bp at the 3′ end of the CDS was amplified using primer pair ishMtAS2-F and ishMtAS2-R (Supplemental Table 2). The PCR product was labeled with digoxigenin (Digoxigenin-11-UTP; Roche Diagnostics) for both sense and antisense probes. The sections of shoot apices of the wild type or the *stf* mutant were processed and hybridized with digoxigenin-labeled probes as described previously (Zhou et al., 2011).

Gene Expression Analysis Assays

For quantitative RT-PCR, total RNAs from unexpanded young leaf tissues of genotype R108, *stf* mutant, and the various transgenic lines were extracted using TRIzol reagent (Invitrogen). Two micrograms of total RNA was reverse transcribed using TaqMan reverse transcription reagent (Invitrogen) in a reaction volume of 100 μL. Quantitative RT-PCR was performed with three biological repeats using SYBR Green real-time PCR Master Mix (Invitrogen). PCR was performed at 95°C for 10 min followed by 40 cycles of 95°C for 15s and 60°C for 1 min. The relative expression level of each gene was calculated using the ddCt method (Lin et al., 2013), and the *M. truncatula ACTIN* gene was used as an internal control.

Accession Numbers

Sequence data from this article can be found in TAIR (http://www.arabidopsis.org), *Medicago truncatula* Information Resource (http://www.medicago.org), or GenBank/EMBL/Phytozome databases under the accession numbers listed in Supplemental Table 3.

Supplemental Data

The following materials are available in the online version of this article.

Supplemental Figure 1. Sequence Alignment of STF with Its Orthologs.

Supplemental Figure 2. Concurrent Mutations in Both WUS Box and STF Box Abolished Complementation of the *M. truncatula stf* Mutant.

Supplemental Figure 3. Sequence Alignment and Phylogenetic Analysis of Mt-TPL and Other Members of the TPL Family Using Full-Length Amino Acid Sequences.

Supplemental Figure 4. STF Interacts with Other TPL Family Proteins from *M. truncatula*.

Supplemental Figure 5. STF Interacts with Mt-TPL and Localizes in the Nucleus.

Supplemental Figure 6. Negative Control for STF Interaction Domain Mapping.

Supplemental Figure 7. Identification of an *M. truncatula* AS2 and Interaction of Mt-AS2 with Mt-AS1.

Supplemental Figure 8. Complementation of *Arabidopsis* Mutants by *M. truncatula* Genes.

Supplemental Figure 9. Silencing of Mt-*AS2* Promotes Leaf Laminar Growth and Partially Complements the *stf* Narrow Leaf Phenotype.

Supplemental Figure 10. Ectopic Expression of Mt-*AS2* in Tobacco Resulted in Adaxialized Narrow Leaves.

Supplemental Table 1. Phenotype of Complementation Assays in *N. sylvestris*.

Supplemental Table 2. Sequences of Primers Used in This Study.

Supplemental Table 3. Accession Numbers or Gene Identifiers of Sequences Used for Multiple Sequence Alignment and Phylogenetic Tree Construction.

Supplemental Data Set 1. Text File of the Alignment Corresponding to Supplemental Figure 3.

ACKNOWLEDGMENTS

We thank Elison Blancaflor and Jin Nakashima for their help with confocal microscopy, Kirankumar Mysore for providing greenhouse space, Yuhai Cui for providing Gateway-compatible Y2H and BiFC vectors, Michiel Vandenbussche for providing *wox1 prs* seeds, Jennifer Fletcher for providing the *as2-1* seeds, Jeffrey A. Long and TAIR for providing the *tpl-1* seeds, Jen Sheen and Lei Li for sharing the protoplast-ChIP protocol, Neil McHale for stimulating discussions, and Randy Allen, Hao Lin, and Lifang Niu for critical reading of the manuscript and stimulating discussions. This work was supported by the Oklahoma Center for the Advancement of Science and Technology (Grant PBS11-002) and the National Science Foundation (Grants EPS-0814361, IOS-1354422, and DBI 0400580).

AUTHOR CONTRIBUTIONS

F.Z. designed the research, performed research, analyzed data, and wrote the article. Y.W., G.L., and Y.T. performed research. E.M.K. analyzed data and edited the article. M.T. designed the research, analyzed data, and wrote the article.

Received December 14, 2013; revised January 28, 2014; accepted February 3, 2014; published February 28, 2014.

REFERENCES

Asai, T., Tena, G., Plotnikova, J., Willmann, M.R., Chiu, W.L., Gomez-Gomez, L., Boller, T., Ausubel, F.M., and Sheen, J. (2002). MAP kinase signalling cascade in Arabidopsis innate immunity. Nature **415:** 977–983.

Bowman, J.L., Eshed, Y., and Baum, S.F. (2002). Establishment of polarity in angiosperm lateral organs. Trends Genet. **18:** 134–141.

Breuninger, H., Rikirsch, E., Hermann, M., Ueda, M., and Laux, T. (2008). Differential expression of WOX genes mediates apical-basal axis formation in the Arabidopsis embryo. Dev. Cell **14:** 867–876.

Byrne, M.E. (2012). Making leaves. Curr. Opin. Plant Biol. **15:** 24–30.

Byrne, M.E., Barley, R., Curtis, M., Arroyo, J.M., Dunham, M., Hudson, A., and Martienssen, R.A. (2000). Asymmetric leaves1 mediates leaf patterning and stem cell function in Arabidopsis. Nature **408:** 967–971.

Causier, B., Ashworth, M., Guo, W., and Davies, B. (2012). The TOPLESS interactome: A framework for gene repression in Arabidopsis. Plant Physiol. **158:** 423–438.

Cho, S.-H., Yoo, S.-C., Zhang, H., Pandeya, D., Koh, H.-J., Hwang, J.-Y., Kim, G.-T., and Paek, N.-C. (2013). The rice narrow leaf2 and narrow leaf3 loci encode WUSCHEL-related homeobox 3A (OsWOX3A) and function in leaf, spikelet, tiller and lateral root development. New Phytol. **198:** 1071–1084.

Du, L., Ali, G.S., Simons, K.A., Hou, J., Yang, T., Reddy, A.S., and Poovaiah, B.W. (2009). Ca^{2+}/calmodulin regulates salicylic-acid-mediated plant immunity. Nature **457:** 1154–1158.

Efroni, I., Eshed, Y., and Lifschitz, E. (2010). Morphogenesis of simple and compound leaves: A critical review. Plant Cell **22:** 1019–1032.

Emery, J.F., Floyd, S.K., Alvarez, J., Eshed, Y., Hawker, N.P., Izhaki, A., Baum, S.F., and Bowman, J.L. (2003). Radial patterning of Arabidopsis shoots by class III HD-ZIP and KANADI genes. Curr. Biol. **13:** 1768–1774.

Guo, M., Thomas, J., Collins, G., and Timmermans, M.C.P. (2008). Direct repression of *KNOX* loci by the ASYMMETRIC LEAVES1 complex of *Arabidopsis*. Plant Cell **20:** 48–58.

Hagemann, W., and Gleissberg, S. (1996). Organogenetic capacity of leaves: The significance of marginal blastozones in angiosperms. Plant Syst. Evol. **199:** 121–152.

Hake, S., Smith, H.M.S., Holtan, H., Magnani, E., Mele, G., and Ramirez, J. (2004). The role of knox genes in plant development. Annu. Rev. Cell Dev. Biol. **20:** 125–151.

Husbands, A.Y., Chitwood, D.H., Plavskin, Y., and Timmermans, M.C. (2009). Signals and prepatterns: New insights into organ polarity in plants. Genes Dev. **23:** 1986–1997.

Ikeda, M., Mitsuda, N., and Ohme-Takagi, M. (2009). *Arabidopsis* WUSCHEL is a bifunctional transcription factor that acts as a repressor in stem cell regulation and as an activator in floral patterning. Plant Cell **21:** 3493–3505.

Iwakawa, H., Iwasaki, M., Kojima, S., Ueno, Y., Soma, T., Tanaka, H., Semiarti, E., Machida, Y., and Machida, C. (2007). Expression of the ASYMMETRIC LEAVES2 gene in the adaxial domain of Arabidopsis leaves represses cell proliferation in this domain and is critical for the development of properly expanded leaves. Plant J. **51:** 173–184.

Iwasaki, M., et al. (2013). Dual regulation of ETTIN (ARF3) gene expression by AS1-AS2, which maintains the DNA methylation level, is involved in stabilization of leaf adaxial-abaxial partitioning in Arabidopsis. Development **140:** 1958–1969.

Ji, J., Strable, J., Shimizu, R., Koenig, D., Sinha, N., and Scanlon, M.J. (2010). WOX4 promotes procambial development. Plant Physiol. **152:** 1346–1356.

Juarez, M.T., Kui, J.S., Thomas, J., Heller, B.A., and Timmermans, M.C. (2004). MicroRNA-mediated repression of rolled leaf1 specifies maize leaf polarity. Nature **428:** 84–88.

Kerstetter, R.A., Bollman, K., Taylor, R.A., Bomblies, K., and Poethig, R.S. (2001). KANADI regulates organ polarity in Arabidopsis. Nature **411:** 706–709.

Kieffer, M., Stern, Y., Cook, H., Clerici, E., Maulbetsch, C., Laux, T., and Davies, B. (2006). Analysis of the transcription factor WUSCHEL and its functional homologue in *Antirrhinum* reveals a potential mechanism for their roles in meristem maintenance. Plant Cell **18:** 560–573.

Kramer, E.M. (2009). Aquilegia: A new model for plant development, ecology, and evolution. Annu. Rev. Plant Biol. **60:** 261–277.

Krogan, N.T., Hogan, K., and Long, J.A. (2012). APETALA2 negatively regulates multiple floral organ identity genes in Arabidopsis by recruiting the co-repressor TOPLESS and the histone deacetylase HDA19. Development **139:** 4180–4190.

Lee, J.H., Yoo, S.J., Park, S.H., Hwang, I., Lee, J.S., and Ahn, J.H. (2007). Role of SVP in the control of flowering time by ambient temperature in Arabidopsis. Genes Dev. **21:** 397–402.

Leibfried, A., To, J.P., Busch, W., Stehling, S., Kehle, A., Demar, M., Kieber, J.J., and Lohmann, J.U. (2005). WUSCHEL controls meristem function by direct regulation of cytokinin-inducible response regulators. Nature **438:** 1172–1175.

Lin, H., Niu, L., McHale, N.A., Ohme-Takagi, M., Mysore, K.S., and Tadege, M. (2013). Evolutionarily conserved repressive activity of WOX proteins mediates leaf blade outgrowth and floral organ development in plants. Proc. Natl. Acad. Sci. USA **110:** 366–371.

Lodha, M., Marco, C.F., and Timmermans, M.C.P. (2013). The ASYMMETRIC LEAVES complex maintains repression of KNOX homeobox genes via direct recruitment of Polycomb-repressive complex2. Genes Dev. **27:** 596–601.

Lohmann, J.U., Hong, R.L., Hobe, M., Busch, M.A., Parcy, F., Simon, R., and Weigel, D. (2001). A molecular link between stem cell regulation and floral patterning in Arabidopsis. Cell **105:** 793–803.

Long, J.A., Ohno, C., Smith, Z.R., and Meyerowitz, E.M. (2006). TOPLESS regulates apical embryonic fate in Arabidopsis. Science **312:** 1520–1523.

Lu, Q., Tang, X., Tian, G., Wang, F., Liu, K., Nguyen, V., Kohalmi, S. E., Keller, W.A., Tsang, E.W., Harada, J.J., Rothstein, S.J., and Cui, Y. (2010). Arabidopsis homolog of the yeast TREX-2 mRNA export complex: Components and anchoring nucleoporin. Plant J. **61:** 259–270.

Luo, M., Yu, C.-W., Chen, F.-F., Zhao, L., Tian, G., Liu, X., Cui, Y., Yang, J.-Y., and Wu, K. (2012). Histone deacetylase HDA6 is functionally associated with AS1 in repression of KNOX genes in Arabidopsis. PLoS Genet. **8:** e1003114.

Matsumoto, N., and Okada, K. (2001). A homeobox gene, PRESSED FLOWER, regulates lateral axis-dependent development of Arabidopsis flowers. Genes Dev. **15:** 3355–3364.

McConnell, J.R., and Barton, M.K. (1998). Leaf polarity and meristem formation in Arabidopsis. Development **125:** 2935–2942.

McConnell, J.R., Emery, J., Eshed, Y., Bao, N., Bowman, J., and Barton, M.K. (2001). Role of PHABULOSA and PHAVOLUTA in determining radial patterning in shoots. Nature **411:** 709–713.

McHale, N.A. (1992). A nuclear mutation blocking initiation of the lamina in leaves of *Nicotiana sylvestris*. Planta **186:** 355–360.

Moon, J., and Hake, S. (2011). How a leaf gets its shape. Curr. Opin. Plant Biol. **14:** 24–30.

Nakata, M., Matsumoto, N., Tsugeki, R., Rikirsch, E., Laux, T., and Okada, K. (2012). Roles of the middle domain-specific *WUSCHEL-RELATED HOMEOBOX* genes in early development of leaves in *Arabidopsis*. Plant Cell **24:** 519–535.

Nardmann, J., Ji, J., Werr, W., and Scanlon, M.J. (2004). The maize duplicate genes narrow sheath1 and narrow sheath2 encode a conserved homeobox gene function in a lateral domain of shoot apical meristems. Development **131:** 2827–2839.

Phelps-Durr, T.L., Thomas, J., Vahab, P., and Timmermans, M.C.P. (2005). Maize rough sheath2 and its *Arabidopsis* orthologue ASYMMETRIC LEAVES1 interact with HIRA, a predicted histone chaperone, to maintain *knox* gene silencing and determinacy during organogenesis. Plant Cell **17:** 2886–2898.

Sarkar, A.K., Luijten, M., Miyashima, S., Lenhard, M., Hashimoto, T., Nakajima, K., Scheres, B., Heidstra, R., and Laux, T. (2007). Conserved factors regulate signalling in *Arabidopsis thaliana* shoot and root stem cell organizers. Nature **446:** 811–814.

Schoof, H., Lenhard, M., Haecker, A., Mayer, K.F., Jürgens, G., and Laux, T. (2000). The stem cell population of Arabidopsis shoot meristems in maintained by a regulatory loop between the CLAVATA and WUSCHEL genes. Cell **100:** 635–644.

Schwab, R., Ossowski, S., Riester, M., Warthmann, N., and Weigel, D. (2006). Highly specific gene silencing by artificial microRNAs in *Arabidopsis*. Plant Cell **18:** 1121–1133.

Shimizu, R., Ji, J., Kelsey, E., Ohtsu, K., Schnable, P.S., and Scanlon, M.J. (2009). Tissue specificity and evolution of meristematic WOX3 function. Plant Physiol. **149:** 841–850.

Soltis, D.E., et al. (2008). The Amborella genome: An evolutionary reference for plant biology. Genome Biol. **9:** 402.

Szemenyei, H., Hannon, M., and Long, J.A. (2008). TOPLESS mediates auxin-dependent transcriptional repression during Arabidopsis embryogenesis. Science **319:** 1384–1386.

Tadege, M., et al. (2011a). *STENOFOLIA* regulates blade outgrowth and leaf vascular patterning in *Medicago truncatula* and *Nicotiana sylvestris*. Plant Cell **23:** 2125–2142.

Tadege, M., Lin, H., Niu, L., and Mysore, K.S. (2011b). Control of dicot leaf blade expansion by a WOX gene, STF. Plant Signal. Behav. **6:** 1861–1864.

Tsukaya, H. (2006). Mechanism of leaf-shape determination. Annu. Rev. Plant Biol. **57:** 477–496.

Ueno, Y., Ishikawa, T., Watanabe, K., Terakura, S., Iwakawa, H., Okada, K., Machida, C., and Machida, Y. (2007). Histone deacetylases and ASYMMETRIC LEAVES2 are involved in the establishment of polarity in leaves of *Arabidopsis*. Plant Cell **19:** 445–457.

Vandenbussche, M., Horstman, A., Zethof, J., Koes, R., Rijpkema, A.S., and Gerats, T. (2009). Differential recruitment of *WOX* transcription factors for lateral development and organ fusion in petunia and *Arabidopsis*. Plant Cell **21:** 2269–2283.

Waites, R., and Hudson, A. (1995). Phantastica: A gene required for dorsoventrality of leaves in *Antirrhinum majus*. Development **121:** 2143–2154.

Waites, R., Selvadurai, H.R.N., Oliver, I.R., and Hudson, A. (1998). The PHANTASTICA gene encodes a MYB transcription factor involved in growth and dorsoventrality of lateral organs in Antirrhinum. Cell **93:** 779–789.

Wang, L., Kim, J., and Somers, D.E. (2013). Transcriptional corepressor TOPLESS complexes with pseudoresponse regulator proteins and histone deacetylases to regulate circadian transcription. Proc. Natl. Acad. Sci. USA **110:** 761–766.

Wu, G., Lin, W.C., Huang, T., Poethig, R.S., Springer, P.S., and Kerstetter, R.A. (2008). KANADI1 regulates adaxial-abaxial polarity in Arabidopsis by directly repressing the transcription of ASYMMETRIC LEAVES2. Proc. Natl. Acad. Sci. USA **105:** 16392–16397.

Xiong, Y., McCormack, M., Li, L., Hall, Q., Xiang, C., and Sheen, J. (2013). Glucose-TOR signalling reprograms the transcriptome and activates meristems. Nature **496:** 181–186.

Zhang, F., Zuo, K.J., Zhang, J.Q., Liu, X.A., Zhang, L.D., Sun, X.F., and Tang, K.X. (2010). An L1 box binding protein, GbML1, interacts with GbMYB25 to control cotton fibre development. J. Exp. Bot. **61:** 3599–3613.

Zhou, C., Han, L., Hou, C., Metelli, A., Qi, L., Tadege, M., Mysore, K.S., and Wang, Z.Y. (2011). Developmental analysis of a *Medicago truncatula smooth leaf margin1* mutant reveals context-dependent effects on compound leaf development. Plant Cell **23:** 2106–2124.

Zhuang, L.-L., Ambrose, M., Rameau, C., Weng, L., Yang, J., Hu, X.-H., Luo, D., and Li, X. (2012). LATHYROIDES, encoding a WUSCHEL-related Homeobox1 transcription factor, controls organ lateral growth, and regulates tendril and dorsal petal identities in garden pea (*Pisum sativum* L.). Mol. Plant **5:** 1333–1345.

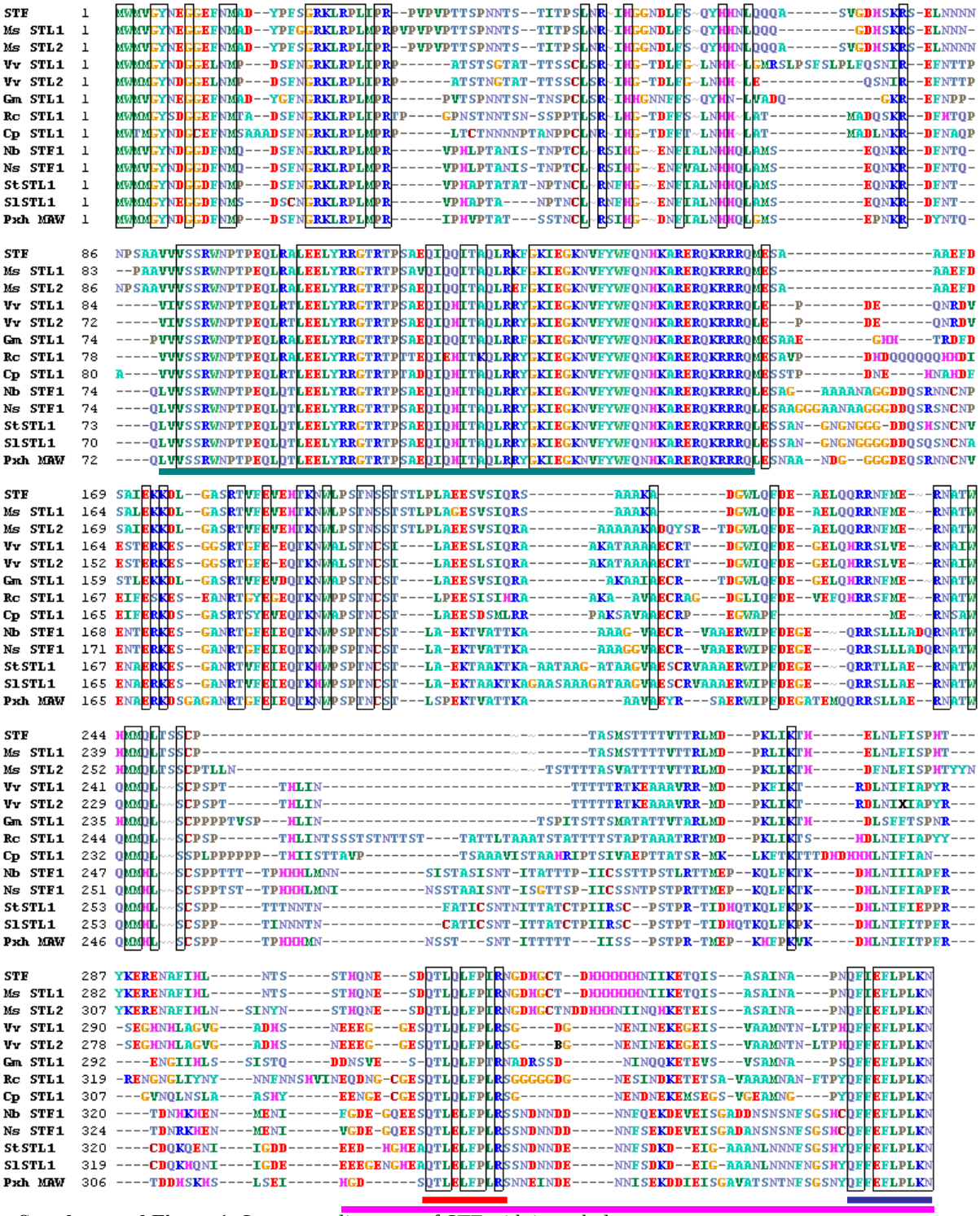

Supplemental Figure 1. Sequence alignment of STF with its orthologs.
Homeodomain (HD), teal; C terminal domain (CTD), pink, includes WUS-box, red; STF-box, blue. NTD is before HD while MD is between HD and CTD.
Ms, *Medicago sativa*; Gm, *Glycine max*; Vv, *Vitis vinifera*; Rc, *Ricinus communis*; Cp, *Carica papaya*; Nb, *Nicotiana benthamiana*; Ns, *Nicotiana sylvestris*; Pxh, *Petunia hybrida*; St, *Solanum tuberosum*; Sl, *Solanum lycopersicum*.

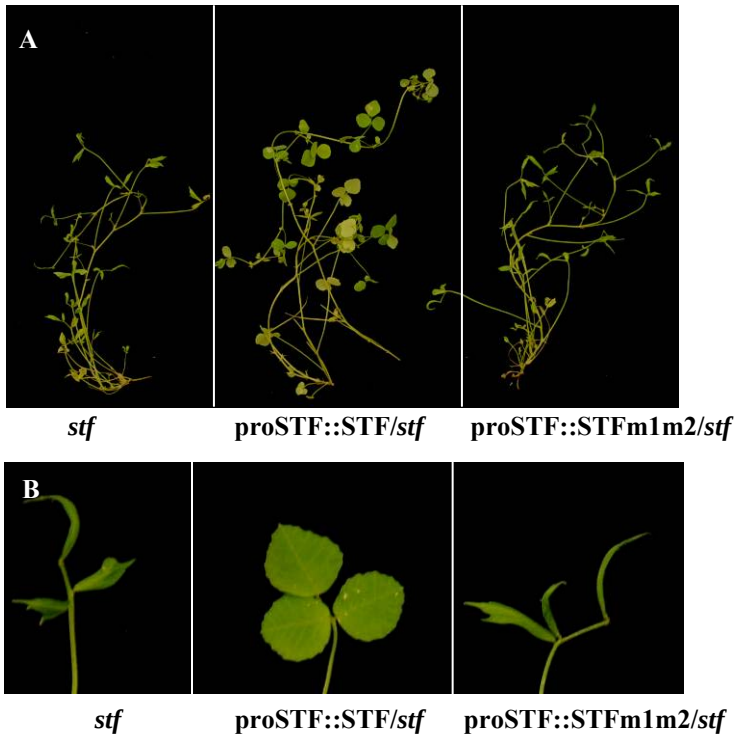

Supplemental Figure 2. Concurrent mutation in both WUS-box and STF-box abolished complementation of *M. truncatula stf* mutant.
(A) *stf* mutant (left), *stf* mutant complemented with pro*STF::STF* construct (middle), and *stf* mutant transformed with pro*STF::STFm1m2* constructs (right).
(B) Close-up view of leaves corresponding to the mutant and transgenic plants in (A).

(A)

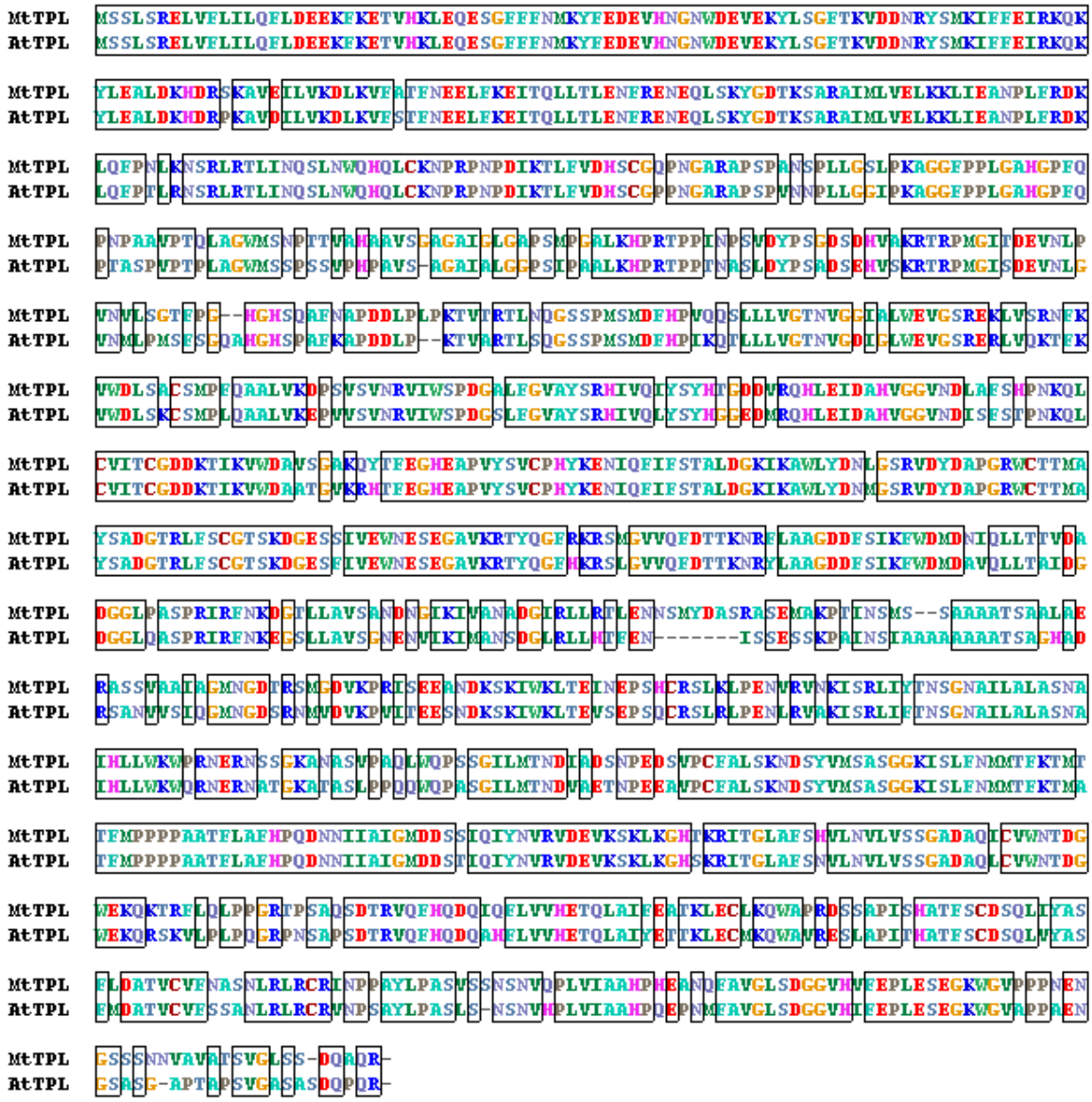

(B)

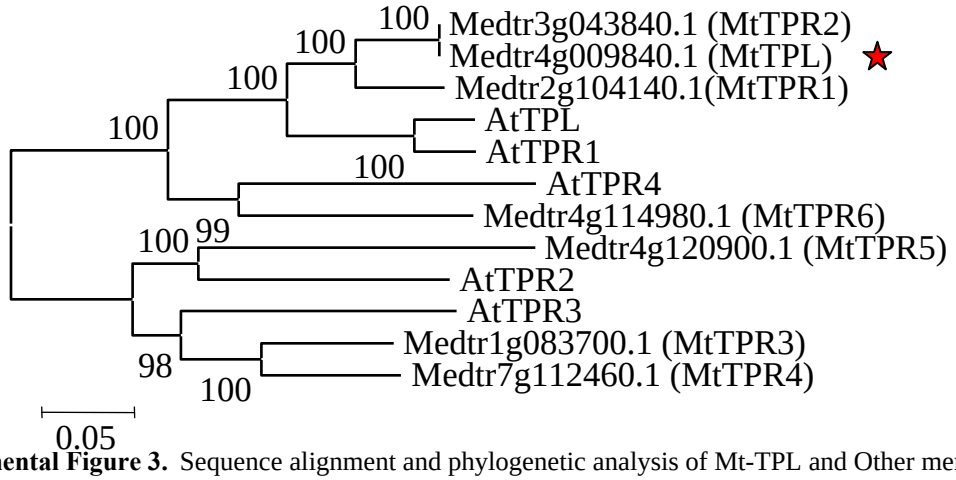

Supplemental Figure 3. Sequence alignment and phylogenetic analysis of Mt-TPL and Other members of the TPL family using full-length amino acid sequences.

(A) Sequence alignment between Mt-TPL and At-TPL. The identical residues were boxed.

(B) Phylogenetic analysis of Medicago and Arabidopsis TPL family members.

Red star highlights the Mt-TPL used in this study. Bootstrap values from 1,000 trials were shown.

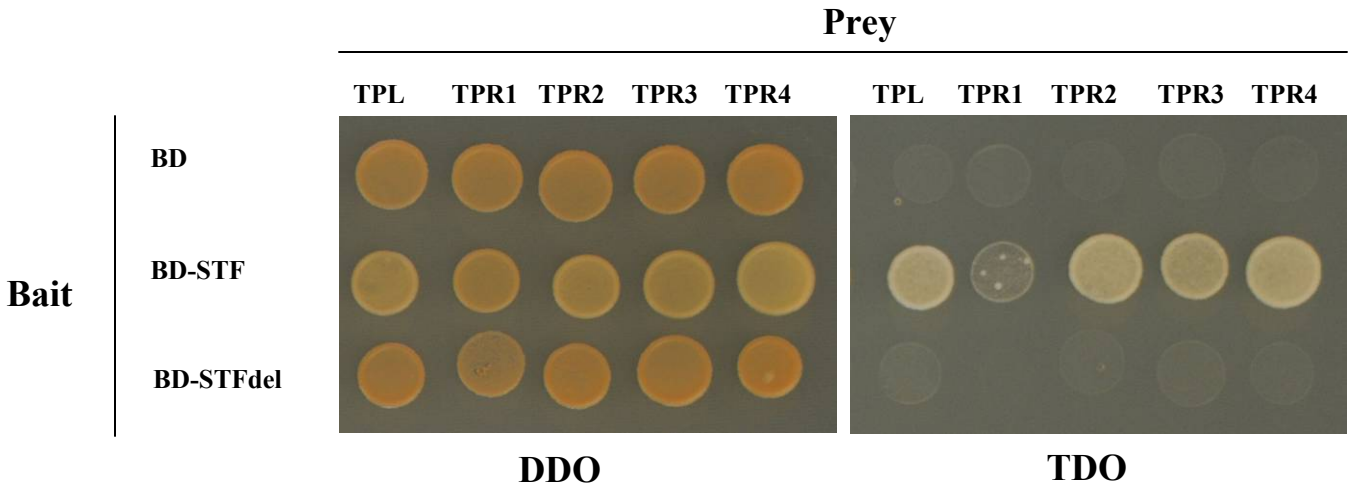

Supplemental Figure 4. STF Interacts with Other TPL Family Proteins from *M. truncatula*

Empty BD vector was used as a negative control for all AD-TPRs. The interaction between STF and TPR proteins was examined by the growth on TDO plates. STFdel which lacks the CTD showed no interaction to any TPR proteins examined supported that the CTD was essential for STF-TPR proteins interaction.

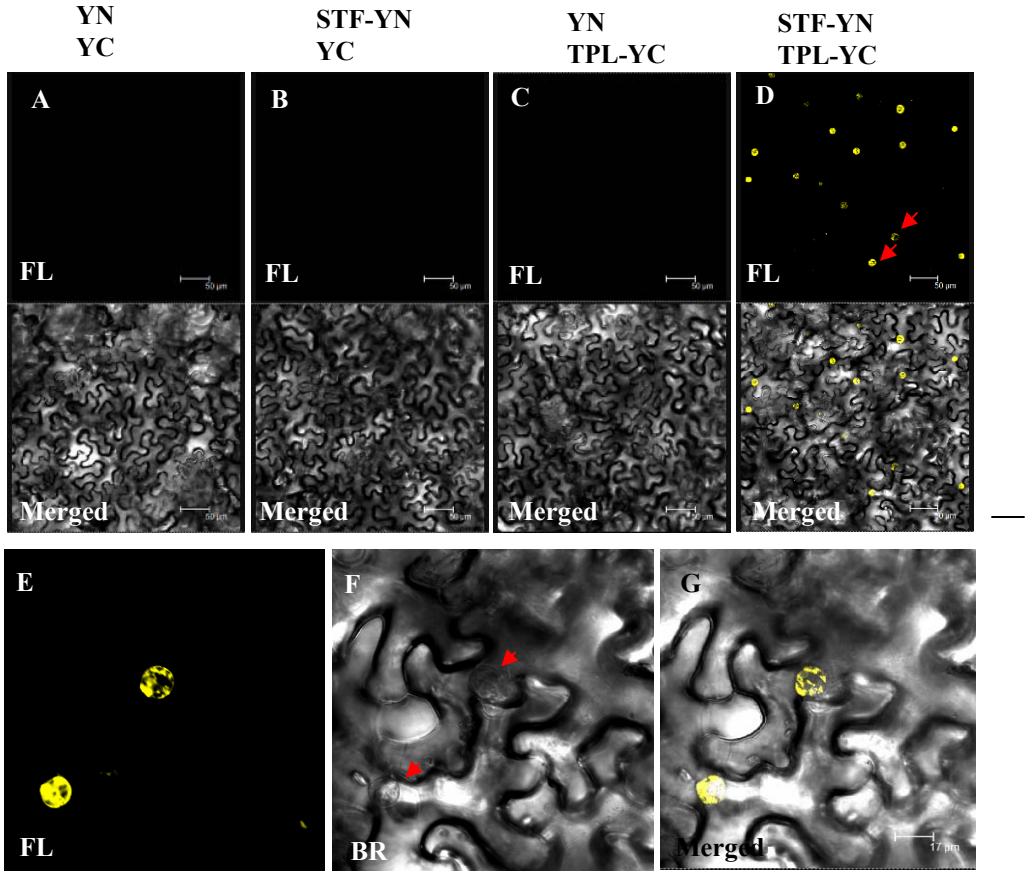

Supplemental Figure 5. STF Interacts with Mt-TPL and localizes in the Nucleus .

(A) Empty YN vector with empty YC vector.
(B) STF-YN vector with empty YC vector.
(C) Empty YN vector with Mt-TPL-YC vector.
(D) STF-YN and Mt-TPL-YC, Arrows point to the nucleus signals which were magnified in **(E)** *to* **(G)**.
(E) STF-YN and Mt-TPL-YC, fluorescence channel.
(F) STF-YN and Mt-TPL-YC, corresponding differential interference contrast (*DIC*) image of **(E)** shows the nucleus pointed by arrows.
(G) STF-YN and Mt-TPL-YC, merged image of **(E)** and **(F)**. FL, Fluorescence channel. BR, Bright field. Merged, fluorescence channel merged with bright field.

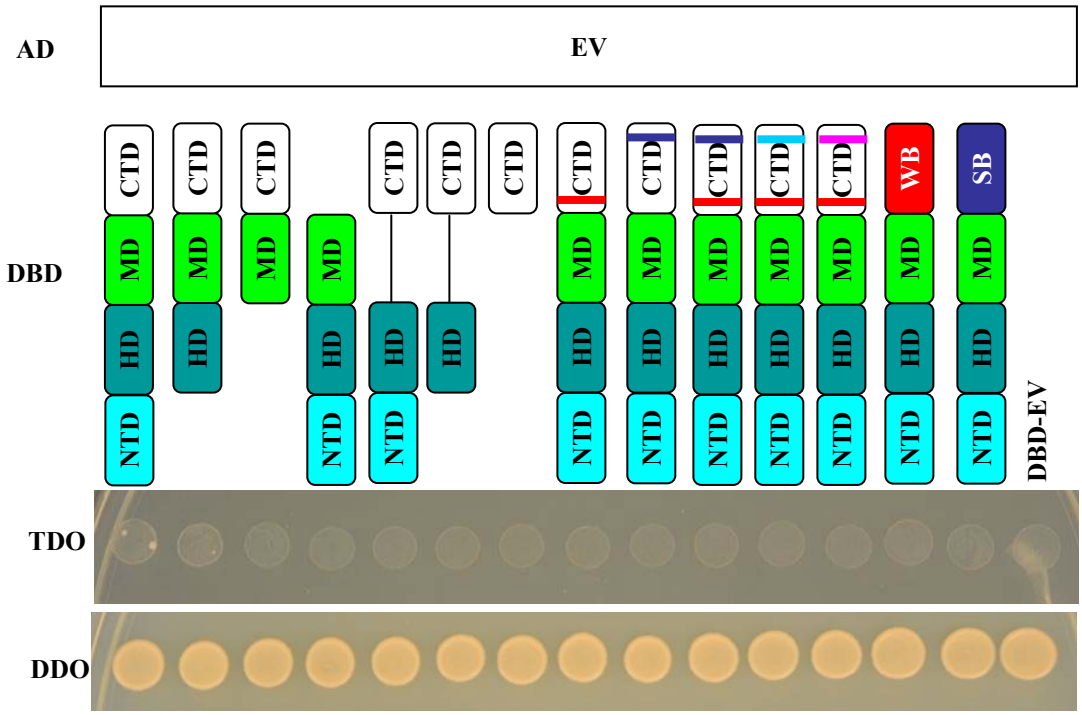

Supplemental Figure 6. Negative control for STF interaction domain mapping.
Different STF mutants were fused to GAL4-DBD domain and co-transformed with empty AD vector. Different point mutations in CTD are showed by lines with different colors. Red, blue, light blue or pink lines represent m1 mutation in WUS-box, m2 mutation in STF-box, m2-L1A mutation in STF-box, or m2-L2A mutation in STF-box, respectively. WB, WUS-box; SB, STF-box, respectively. EV stands for empty vector. Representative data are shown from three repeats.

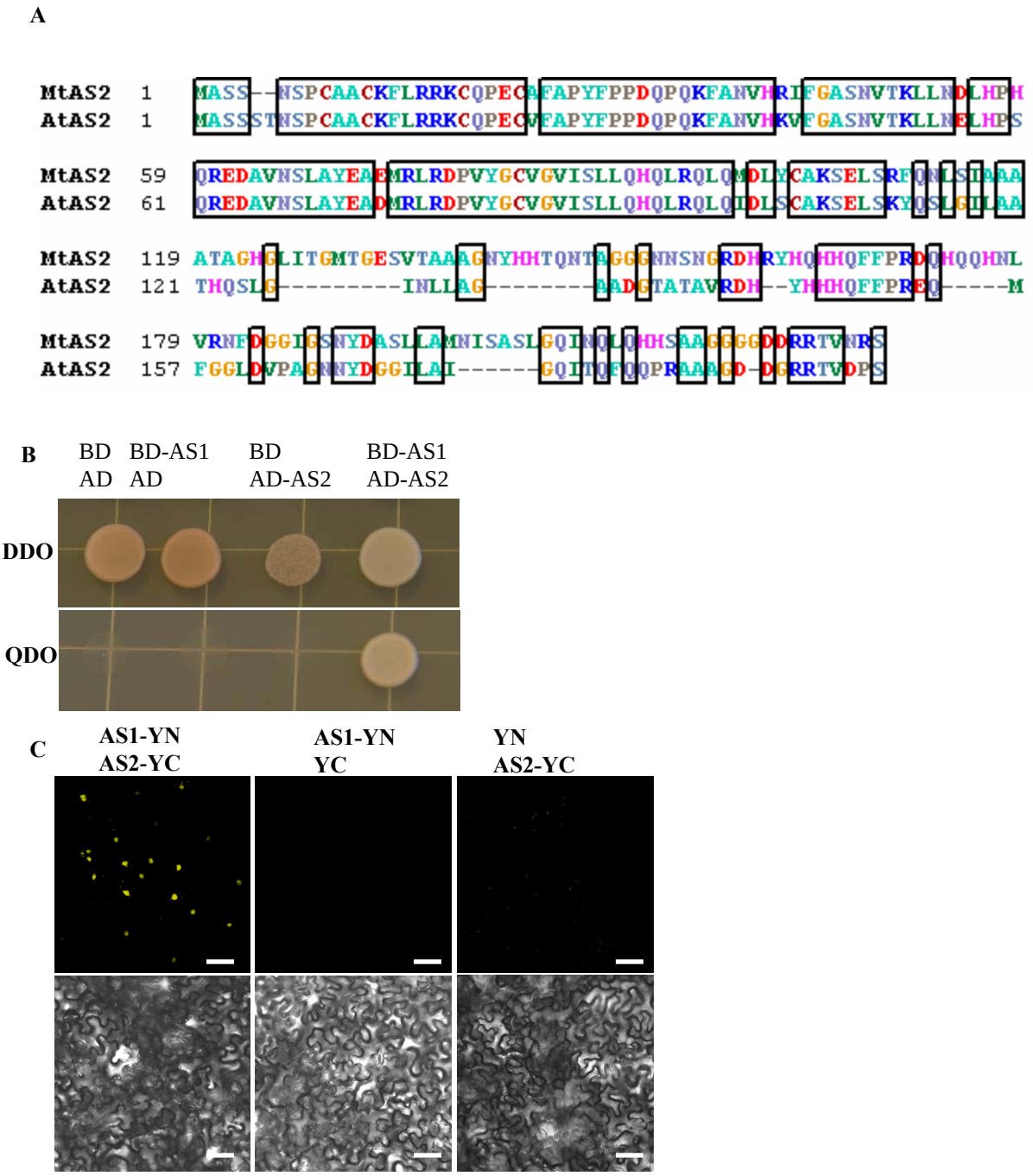

Supplemental Figure 7. Identification of a *M. truncatula* AS2 and Interaction of Mt-AS2 with Mt-AS1.
(A) Protein sequence alignment of AS2 proteins from Arabidopsis thaliana (At-AS2) and M. truncatula (Mt-AS2).
(B) Yeast two-hybrid showed that Mt-AS2 interacts with Mt-AS1.
(C) BiFC assay showed that Mt-AS2 interacts with Mt-AS1 in plant cells. Bars=50 μm.

Supplemental Figure 8. Complementation of *Arabidopsis thaliana* mutants by *M. truncatula* genes

(A) Arabidopsis *as2-1* asymmetric leaf phenotype (left, asymmetric leaves indicated by white arrows) was rescued by the expression of MtAS2 protein under Medicago *AS2* promoter (*proAS2:AS2*, right)

(B) Arabidopsis *wox1 prs* mutant (left) was rescued by the expression of STF-YFP fusion protein under *STF* promoter (*proSTF:STF-YFP*, right)

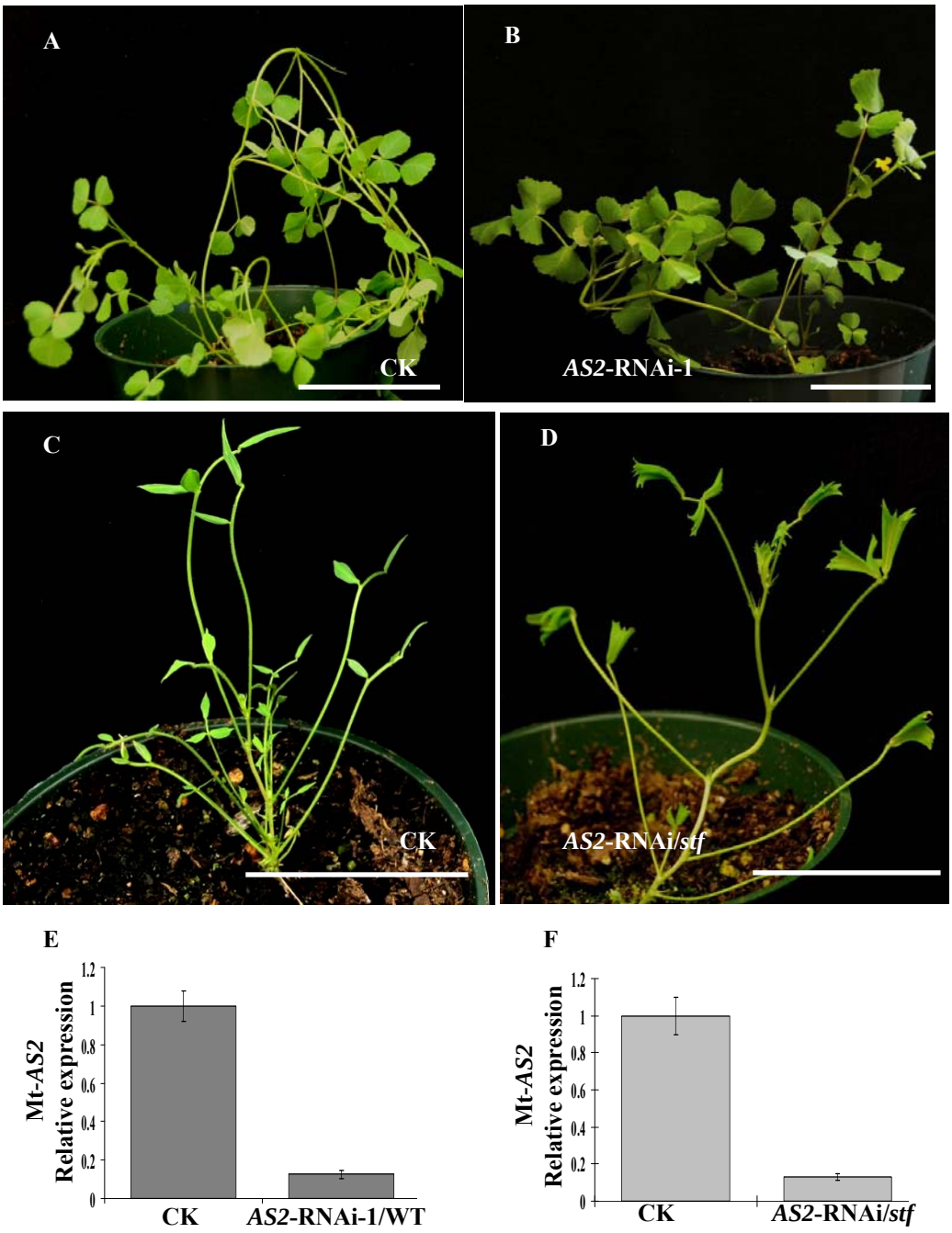

Supplemental Figure 9. Silencing of Mt-*AS2* promotes leaf laminar growth and partially rescued stf narrow leaf phenotype
(A) Control plant for R108 (Plants genotyped as negative from the same stage of transgenic plants were used as CK)
(B) Mt-*AS2*-RNAi line 1, Leaves showed down-curling and wider blade than control plants.
(C) Control plant for *stf* (Plants genotyped as negative from the same stage of transgenic plants were used as CK)
(D) One representative Mt-*AS2*-RNAi plant in stf background, Leaves showed down-curling, more serrations and also partial rescue of *stf* narrow leaf phenotypes.
(E) Real-time PCR analysis of Mt-AS2 expression level in CK and Mt-AS2-RNAi-1 plants.
(F) Real-time PCR analysis of Mt-AS2 expression level in CK and Mt-AS2-RNAi/*stf* plants.
Bars=5 cm.

Supplemental Figure 10 Ectopic expression of Mt-*AS2* in tobacco resulted in adaxialized narrow leaves

Supplemental Table 1. Phenotype of complementation assays in *Nicotiana sylvestris*

STF proteins	width of the biggest leaves (cm)					wavy leaf	plants
	>6	4-6	2-4	0.5-2	<0.5 (no)	margin	examined
STF	22	18	2	0	0	10	42
HD-MD-CTD	3	17	14	2	0	29	36
NTD-HD-CTD	0	24	12	0	0	34	36
STF HD-CTD	0	5	26	5	0	36	36
STF MD-CTD	0	0	0	0	18	NA	18
STFdel	0	0	0	0	18	NA	18
SRDX-STFdel	4	20	12	0	0	26	36
STFm1	0	15	18	3	0	36	36
STFm2	0	8	21	7	0	36	36
STFm1m2	0	0	0	0	18	NA	18
STFdel-WB	0	4	8	24	0	36	36
STFdel-SB	0	10	15	11	0	36	36
STFm1-m2L1A	0	0	0	0	36	NA	36
STFm1-m2L2A	0	0	0	36	0	36	36
STFm1L1A-m2	0	0	0	0	36	NA	18
STFm1L2A-m2	0	0	0	0	36	NA	18
STFm3	0	0	0	0	18	NA	18
STFdel-TPL	3	12	19	2	0	36	36
TPL	0	0	0	0	18	NA	18

Plants were measured after 6 wk of growth in the greenhouse. The biggest leaf of each plant was measured for its width and the smoothness of leaf margin.

Supplemental Table 2. Sequences of primers used in this study.

Primer name	Sequence
Deletion assay	
STF-attB1	GGGGACAAGTTTGTACAAAAAAGCAGGCTTCATGTGGATGGTGGGTTACAAT
STF-91-attB1	GGGGACAAGTTTGTACAAAAAAGCAGGCTTCATGGTTGTGGTGAGTTCAAGATGG
STF-164-attB1	GGGGACAAGTTTGTACAAAAAAGCAGGCTTCATGGCTGCTGAGTTTGATTCTGC
STF-301-attB1	GGGGACAAGTTTGTACAAAAAAGCAGGCTTCAGTACTCATCAAAATGAATCTGATC
STF-163-attB2	GGGGACCACTTTGTACAAGAAAGCTGGGTCTCAAGCTGCTGATTCCATTTGAC
STF-300-attB2	GGGGACCACTTTGTACAAGAAAGCTGGGTCTCAACTAGTATTTAAGTGGATAAAAG
STF-stop-attB2	GGGGACCACTTTGTACAAGAAAGCTGGGTCTCAGTTTTTCAAGGGAAGAAACT
163-301-F	GCGTCAAATGGAATCAGCAAGTACTCATCAAAATGAATCT
163-301-R	AGATTCATTTTGATGAGTACTTGCTGATTCCATTTGACGC
MtTPL-350-R	GGGGACCACTTTGTACAAGAAAGCTGGGTCTCACGTGACAGTCTTCGGCAATGGC
MtTPL-93-F	
Point mutation	mutated sites are indicated by red and lowercase
STFm1-F	AATCTGATCAAACC**gcc**CAA**gct**TTCCCAATAAGGAATG
STFm1-R	CATTCCTTATTGGGAA**agc**TTG**ggc**GGTTTGATCAGATT
STFm1L1-F	AATCTGATCAAACC**gcc**CAACTTTTCCCAATAAGGAATG
STFm1L1-R	CATTCCTTATTGGGAAAAGTTG**ggc**GGTTTGATCAGATT
STFm1L2-F	AATCTGATCAAACCCTTCAA**gct**TTCCCAATAAGGAATG
STFm1L2-R	CATTCCTTATTGGGAA**agc**TTGAAGGGTTTGATCAGATT
STFm2-R1	TCAGTTTTT**tgc**GGG**tgc**AAACTCAATA
STFm2-R2-attB2	GGGGACCACTTTGTACAAGAAAGCTGGGTCTCAGTTTTT**tgc**GGG**tgc**AAACTCAATA
STFm2L1A-attB2	GGGGACCACTTTGTACAAGAAAGCTGGGTCTCAGTTTTTCAAGGG**tgc**AAACTC
STFm2L2A-attB2	GGGGACCACTTTGTACAAGAAAGCTGGGTCTCAGTTTTT**tgc**GGGAAGAAACTCAAT
STFm3-F	TCTATTGGTTTCAGA**t**TCACAAAGC
STFm3-R	GCTTTGTGA**t**TCTGAAACCAATAGA
MtTPL-m1-F	CTTAAAAACTCAAGGTTAAGGACACTCATC**c**ATCAAAGCTTGAATTGGCAGCATCAAC
MtTPL-m1-R	TAGTTGATGCTGCCAATTCAAGCTTTGAT**g**GATGAGTGTCCTTAACCTTGAGTTTTTAA
Protein expression	
STF-*Nco*I	CCATGGGAATGTGGATGGTGGGTTACAAT
STF-*Hin*dIII	AAGCTTTCAGTTTTTCAAGGGAAGAAACT
Protein Fusion	
SRDX-STF-F	ATGGATCTGGATCTAGAACTCCGTTTGGGTTTCGCCCCGATGTGGATGGTGGGTTACAA
SRDX-attB1	GGGGACAAGTTTGTACAAAAAAGCAGGCTTCATGGATCTGGATCTAGAACTC
300-WUS-box-R	ATTCCTTATTGGGAAAAGTTGAAGGGTTTGATCAGAACTAGTATTTAAGTGGATAAAA
WUS-box-attB2	GGGGACCACTTTGTACAAGAAAGCTGGGTCTCAATTCCTTATTGGGAAAAGTTGAAG
300-STF-box-R	GTTTTTCAAGGGAAGAAACTCAATAAACTGGTTGGGACTAGTATTTAAGTGGATAAAA
STF-*Sal*I-F	GAGAGTCGACATGTGGATGGTGGGTTACAAT
STF-300-*Eco*RI-no stop	GGATCCTCAACGGCGATCTTGCTTAGACTT
MtTPL-*Eco*RI-F	GAATTCATGTCATCTCTGAGTAGGGAATTG
MtTPL-*Not*I-R	GCGGCCGCTCATCTTTGTGCTTGGTCTGAAG
MtTPL-attB2	GGGGACCACTTTGTACAAGAAAGCTGGGTCTCATCTTTGTGCTTGGTCTGAAG
MtTPL-attB1	GGGGACAAGTTTGTACAAAAAAGCAGGCTTCATGTCATCTCTGAGTAGGGAATTG
MtTPL-no stop	GGGGACCACTTTGTACAAGAAAGCTGGGTCTCTTTGTGCTTGGTCTGAAG
STF-no stop-attB2	GGGGACCACTTTGTACAAGAAAGCTGGGTCGTTTTTCAAGGGAAGAAACT
STF-m2-no stop	GGGGACCACTTTGTACAAGAAAGCTGGGTCGTTTTTTGCGGGTGCAAACTCAATA
MtAS2-no stop	GGGGACCACTTTGTACAAGAAAGCTGGGTCGGAGCGGTTAACAGTAC

MtAS1-no stop	GGGGACCACTTTGTACAAGAAAGCTGGGTC**T**CTTCCATTTGATTCAGCATG
Cloning	
MtTPR3-F	GGGGACAAGTTTGTACAAAAAAGCAGGCTTCATGACTTCGTTGAGTAGAGAATTGG
MtTPR3-R	GGGGACCACTTTGTACAAGAAAGCTGGGTCTTATCGTTGGGCCTGATCCGCTG
MtTPR4-F	GGGGACAAGTTTGTACAAAAAAGCAGGCTTCATGACTTCTTTGAGCAGAGAATTGG
MtTPR4-R	GGGGACCACTTTGTACAAGAAAGCTGGGTCTTATCTTTGTGTACCCTGATCGGGTG
MtAS2-F	GGGGACAAGTTTGTACAAAAAAGCAGGCTTCATGGCATCCTCAAATTCACC
MtAS2-R	GGGGACCACTTTGTACAAGAAAGCTGGGTCCTAGGAGCGGTTAACAGTAC
ProMtAS2-F	GGGGACAAGTTTGTACAAAAAAGCAGGCTTCATCCCAAACCAACCACTAGACCAAC
ProMtAS2-R	GGGGACCACTTTGTACAAGAAAGCTGGGTCGGTAGTTTGTTTTTGTCACACAAAC
MtAS1-F	GGGGACAAGTTTGTACAAAAAAGCAGGCTTCATGTCGGATATGAAAGATAGGCAG
MtAS1-R	GGGGACCACTTTGTACAAGAAAGCTGGGTCCTATCTTCCATTTGATTCAGCATG
AtAS2-F	GGGGACAAGTTTGTACAAAAAAGCAGGCTTCATGGCATCTTCTTCAACAAACTCAC
AtAS2-R	GGGGACCACTTTGTACAAGAAAGCTGGGTCTCAAGACGGATCAACAGTACGGCG
ProWUS-F	aaaagcttGGGACGGGTAAAGAAATTACAGAACGGG
ProWUS-R	aaggtaccGTGTGTTTGATTCGACTTTTGTTCAC
EMSA and ChIP assays	
ProMtAS2-p1-F	GTTGATTTGGTTCAATAATAGTCAC
ProMtAS2-p1-R	TCCTCCTCCAATTGTGTCAGTC
ProMtAS2-p2-F	ACCAAACAATTGAGATATAGTAAATG
ProMtAS2-p2-R	GTCGTTGAACTTGAATGAATATC
ProMtAS2-p3-F	TTGATGTATTGGAAACTTGTGTGTC
ProMtAS2-p3-R	CAAAAATAACTAGCAAGAATGTGG
ProMtAS2-p4-F	GAAAGGAAAAGAGTGTGTGTG
ProMtAS2-P4-R	GGTAGTTTGTTTTTGTCACACAAAC
MtAS2-CDS-F	TGGAATTGGGAGCAACTATG
MtAS2-CDS-R	TAACAGTACGGCGGTCGTC
AtActin2-F	CTCAGCACCTTCCAACAGATGTGGA
AtActin2-R	CCAAAAAAATGAACCAAGGACCAAA
Realtime PCR	
qMtAS2-F	TGGAATTGGGAGCAACTATG
qMtAS2-R	TATTACCTATAGCATTAGAAACCCT
qActin-F	TCAATGTGCCTGCCATGTATGT
qActin-R	ACTCACACCGTCACCAGAATCC
In situ	
IshMtAS2-F	AAACTTGAGTATCGCAGCGGCA
IshMtAS2-R	ACCACCAGCAGCACTATGATGT
T7-sense	GCGTAATACGACTCACTATAGGGAAACTTGAGTATCGCAGCGGCA
T7-antisense	GCGTAATACGACTCACTATAGGGACCACCAGCAGCACTATGATGT
ProMtAS2-mini35SSS	
35S-F	CGGAAGACCCTTCCTCTATATAAGGAAGTTCATTTCATTTGGAGAGGACACGCTG
35S-R	CAGCGTGTCCTCTCCAAATGAAATGAACTTCCTTATATAGAGGAAGGGTCTTCCG
ProMtAS2-35-R	TAGAGGAAGGGTCTTCCGGGTAGTTTGTTTTTGTCACACAAAC
35S-R-final	CAGCGTGTCCTCTCCAAATG

Supplemental Table 3. Accession numbers or gene identifiers of sequences used for multiple sequence alignment and phylogenetic tree construction.

Mt-STF	JF276252	Mt-TPL	KC525957
Ms-STL1	AEL30894.1	Mt-TPR1	Medtr2g104140.1
Ms-STL2	AEL30895.1	Mt-TPR2	Medtr3g043840.1
Gm-STL1	XP_003530958	Mt-TPR3	Medtr1g083700.1
Gm-STL2	XP_003525189	Mt-TPR4	Medtr7g112460.1
Ps-LATH	AFQ69082	Mt-TPR5	Medtr4g120900.1
Lj-NAO1	AFQ69083	Mt-TPR6	Medtr4g114980.1
Csi-STL1	orange1.1g039144m.g	Mt-AS1	Medtr7g061550.1
Vv-STL1	XP_002278336	Mt-AS2	KF150768
Vv-STL2	CBI15564	At-TPL	At1g15750
Rc-STL1	XP_002532093	At-TPR1	At1g80490
Ns-LAM1	AEL30893	At-TPR2	At3g16830
Pxh-MAW	ACA64093	At-TPR3	At5g27030
St-STL1	XP_006341531	At-TPR4	At3g15880
Sl-STL1	XP_004235799	At-AS2	AT1G65620
Pt-STL1	XP_002322100	Mt-*AS2* promoter	KF150770
Pt-STL2	XP_002317877		
Aq-STL1	Aquca_091_00003.1		
Mg-STL1	mgv1a021220m		
Al-WOX1	XP_002862807		
At-WOX1	AT3G18010		
Amt-STL1	ERM94101		